

Bring My Cup! Personalizing Vision-Language-Action Models with Visual Attentive Prompting

Sangoh Lee¹ Sangwoo Mo^{2,†} Wook-Shin Han^{1,†}

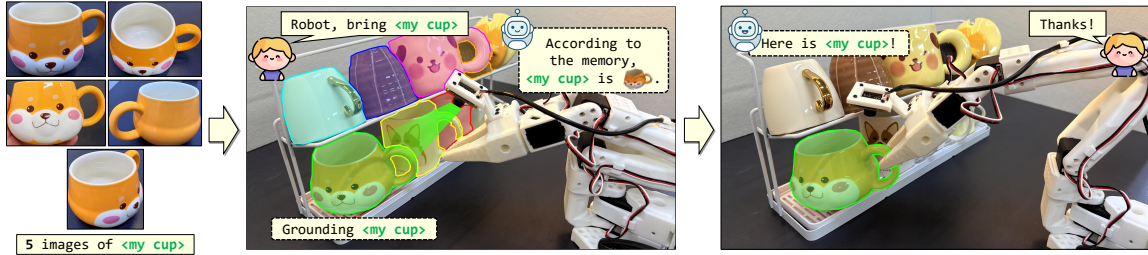


Figure 1. Manipulating personal objects with VLA. Existing vision-language-action (VLA) models cannot handle personal objects such as `<my cup>`, because they can only interpret generic, language-expressible semantics. We address this limitation with a simple framework, Visual Attentive Prompting (VAP). It first grounds the user-specific object in the scene by matching it against the memory and then uses visual prompting to guide the VLA. This pipeline enables existing VLA models to manipulate personal objects without any additional training.

Abstract

While Vision-Language-Action (VLA) models generalize well to generic instructions, they struggle with personalized commands such as “bring my cup,” where the robot must act on one specific instance among visually similar objects. We study this setting of manipulating personal objects, in which a VLA must identify and control a user-specific object unseen during training using only a few reference images. To address this challenge, we propose Visual Attentive Prompting (VAP), a simple-yet-effective training-free perceptual adapter that equips frozen VLAs with top-down selective attention. VAP treats the reference images as a non-parametric visual memory, grounds the personal object in the scene through open-vocabulary detection and embedding-based matching, and then injects this grounding as a visual prompt by highlighting the object and rewriting the instruction. We construct two simulation benchmarks, Personalized-SIMPLER and Personalized-VLABench, and a real-world tabletop benchmark to evaluate personalized manipulation across multiple robots and tasks. Experiments show that VAP consistently outperforms generic policies and token-learning baselines in

both success rate and correct-object manipulation, helping to bridge the gap between semantic understanding and instance-level control.

1. Introduction

“Robot, bring my cup.” You may ask for your coffee mug while getting ready for work, or have the robot fetch your pet’s favorite toy from the living room floor. As illustrated in Figure 1, such scenarios where a user’s personal belongings are mixed with visually similar objects will be a frequent necessity in daily life. To truly assist the user, the robot must discern the subtle visual details that distinguish a specific possession from other counterparts. However, general-purpose policies, such as Vision-Language-Action (VLA) models, typically fail to meet this requirement. Since user-specific instances and the personalized instructions used to refer to them (e.g., “my cup”) are rarely covered during training, these models frequently collapse to category-level recognition and mis-ground the intended instance among same-category distractors.

Recent advancements in robot learning have empowered general-purpose policies to execute diverse manipulation tasks specified by natural language commands (Brohan et al., 2023; Kim et al., 2024; Intelligence et al., 2025). By training on large-scale robot datasets (O’Neill et al., 2023), these models achieve strong generalization to generic instructions (e.g., “pick up the cup”). However, relying solely on language creates a fundamental bottleneck for personalized assistance. Natural language inherently abstracts rich visual details into broad semantic categories. A standard

[†]Equal advising ¹GSAI, POSTECH ²IME, POSTECH. Correspondence to: Sangoh Lee <solee@dblab.postech.ac.kr>.

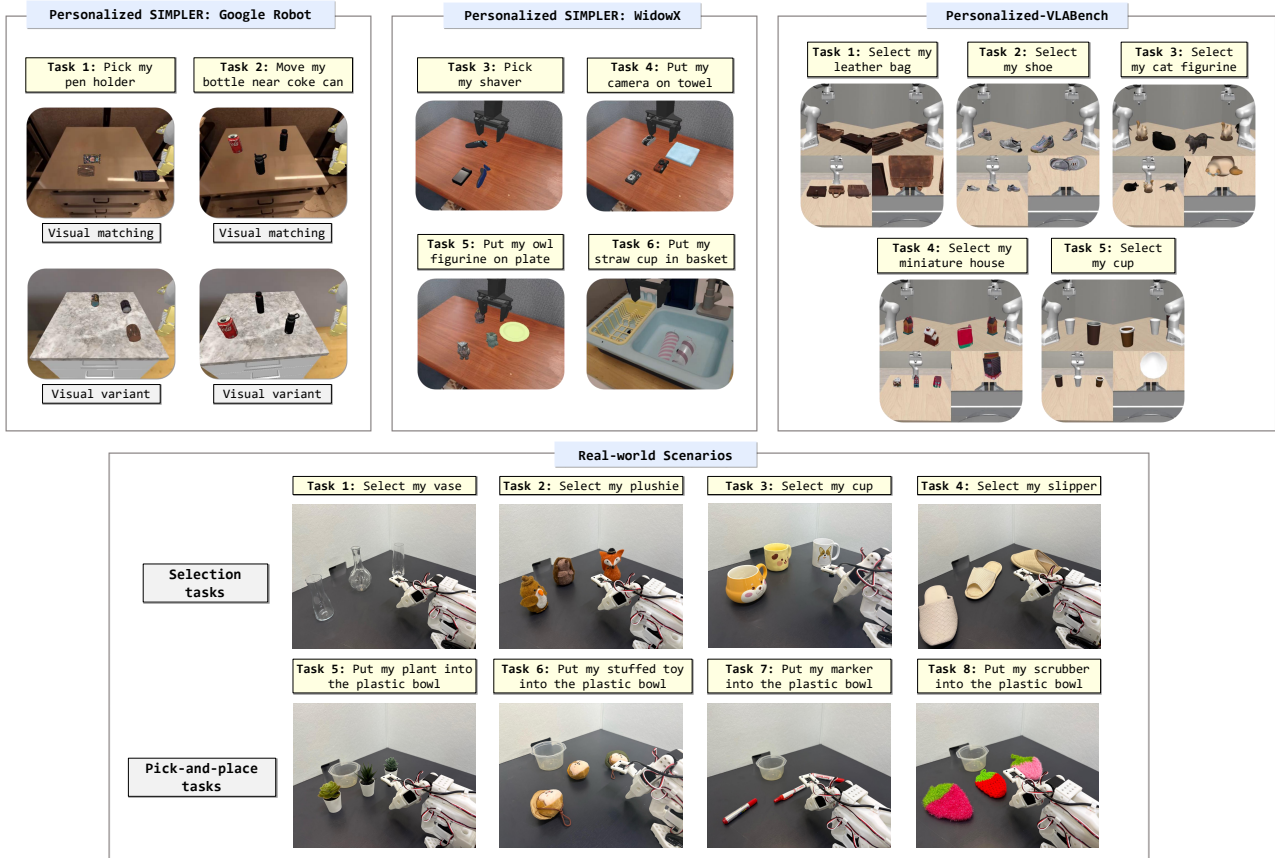


Figure 2. **Overview of Evaluation Benchmarks.** We evaluate our method across simulation and real-world tasks. **Top (Simulation):** We construct *Personalized-SIMPLER* (left/middle) and *Personalized-VLABench* (right) by repopulating existing environments with user-specific assets. **Bottom (Real-world):** We conduct physical experiments on a SO-101 arm using 8 diverse object categories, covering both selection and pick-and-place tasks. In all scenarios, the agent must identify a specific target instance among visually similar distractors, requiring precise instance-level grounding beyond generic category recognition.

VLA interprets a specific request for “my cup” simply as “a cup,” effectively ignoring instance-level distinctions. This generalization leads the model to discard specific nuances, such as a unique pattern or a chip on the rim, that are critical for identifying the target among distractors. Even with detailed descriptions, text-only disambiguation remains brittle for VLAs because fine-grained instance cues must be grounded indirectly through language, as we demonstrate in Sec. 5. Moreover, per-object fine-tuning would require additional data and optimization for each personal item, which is impractical at deployment.

To bridge this semantic gap, we formulate the challenge of manipulating personal objects. Our goal is to adapt a frozen VLA to recognize and control a user’s unique item unseen during training, utilizing only a handful of reference images. Specifically, given a small set of reference views (e.g., 4–5 images), the agent must discern the specific target from visually similar distractors in a cluttered scene. This formulation targets precise instance-level generalization, extending VLA capabilities beyond broad category-

level recognition.

We address this challenge by equipping frozen VLAs with top-down attention in the cognitive sense, namely a mechanism for allocating focus to task-relevant visual evidence at the input level. We propose **Visual Attentive Prompting (VAP)**, a framework that injects instance-awareness into frozen VLAs. VAP bypasses the need for parameter updates by reformulating personalization as a two-stage inference process: (1) **Grounding**, where the system identifies the user’s object using reference images, and (2) **Visual Prompting**, where this grounded knowledge is overlaid directly onto the robot’s observation. By explicitly highlighting the target in pixel space, VAP provides a direct visual focus signal to a frozen policy, enabling it to manipulate the user’s object without relying on language-only disambiguation. As a result, a new personal object can be used immediately after it is registered with a few reference images, without any retraining or fine-tuning.

We validate the efficacy of VAP across a comprehen-

sive suite of simulation and real-world scenarios. Since standard VLA benchmarks primarily evaluate category-level generalization, we establish two new benchmarks, *Personalized-SIMPLER* and *Personalized-VLABench*, designed to rigorously test instance-level identification among distractors (Figure 2, Top). Crucially, to demonstrate practical applicability, we extend this evaluation to a physical robot setup, tasking the agent with manipulating diverse personal objects in real-world (Figure 2, Bottom). Our extensive experiments show that VAP significantly outperforms both generic policies and other personalization baselines, confirming that visual attentive prompting is a robust strategy for bridging the gap between semantic understanding and instance-level control.

Our main contributions are as follows:

- **Personal Object Manipulation:** We introduce a personalization task where an agent must manipulate user-specific objects among visually similar distractors using only a few reference images.
- **Visual Attentive Prompting (VAP):** We propose VAP, a training-free framework that adapts frozen VLAs by translating personal concepts into visual prompts for precise instance-level control, enabling immediate use upon registering new objects.
- **Benchmarks and Evaluation:** We establish two simulation benchmarks and a real-world setup, demonstrating that VAP significantly outperforms generic and other baselines in personalized manipulation.

2. Related Work

VLA Models. Recent advancements have established VLA models as a dominant paradigm for general-purpose robotic manipulation (Kawaharazuka et al., 2025; Wen et al., 2024). By integrating large language models with visual encoders, VLAs such as RT-2 (Brohan et al., 2023), OpenVLA (Kim et al., 2024), Octo (Octo Model Team et al., 2024), GR00T N1.5 (NVIDIA, 2025), π_0 (Black et al., 2024), $\pi_{0.5}$ (Intelligence et al., 2025) and $\pi_{0.6}^*$ (Physical Intelligence et al., 2025) enable a single policy to execute diverse instructions. These models rely on massive robot datasets (O’Neill et al., 2023; Khazatsky et al., 2024; Walke et al., 2023; Fang et al., 2023) to generalize to novel objects and semantic commands. However, recent benchmarks reveal that VLAs often fail at fine-grained visual grounding and degrade significantly under distribution shifts (Fang et al., 2025; Zhang et al., 2025). In personalization, this makes it hard to identify the correct instance among lookalikes and to handle previously unseen personal objects for user-specific references. In this work, we investigate adapting these frozen backbones to personalized scenarios without architectural modifications.

Personalization in Foundation Models. Personalization has emerged as a central theme across foundation models, aiming to adapt large-scale priors to specific user needs. In Large Language Models (LLMs), work has focused on personalized adapters (Tan et al., 2024) and long-term memory banks (Zhong et al., 2024) that align behavior with individual preferences. In the visual domain, text-to-image personalization spans *token optimization* methods such as Textual Inversion (Gal et al., 2022), *weight tuning* techniques like DreamBooth (Ruiz et al., 2023) and Custom Diffusion (Kumari et al., 2023), and more recent *encoder-based* approaches such as IP-Adapter (Ye et al., 2023) and PhotoMaker (Li et al., 2024b) for instant customization. Methods like PerSAM (Zhang et al., 2024) extend this capability to segmentation models, enabling SAM to localize user-designated concepts from a single reference image. Similar ideas have been explored in Vision-Language Models (VLMs), where approaches such as MyVLM (Alaluf et al., 2024) and Yo’LLaVA (Nguyen et al., 2024) apply concept learning to personalized dialogue. Collectively, these works establish personalization as a standard capability in generative models, yet its use remains largely confined to static generation or text-based reasoning, leaving a gap in the embodied control.

Personalization for Robotic Manipulation. Extending personalization to embodied agents introduces additional challenges, as user-specific information must be integrated directly into the robot’s decision-making. Recent works primarily adapt *instruction modalities* or *high-level planning*. VLAS (Zhao et al., 2025) incorporates speech recognition to handle user-specific voice commands. TidyBot (Wu et al., 2023) and ProVox (Grannen et al., 2025) customize task scheduling to user preferences, while MEMENTO (Kwon et al., 2025) studies how agents exploit episodic memory for user-specific object semantics and behavioral patterns. Relatedly, PIN (Barsellotti et al., 2024) conditions an agent on reference images (and a short textual description) of a particular instance to navigate to the target. However, these approaches largely overlook the *control* gap: enabling a general-purpose policy to physically manipulate a specific target instance (e.g., “my cup”) among visually similar distractors using fine-grained visual cues. Our work addresses this gap by using reference images to construct test-time visual prompts that let a frozen, language-conditioned VLA manipulate the correct instance under personalized commands.

Visual Prompting and Grounded Priors. Visual prompting modifies input images (e.g., with bounding boxes, masks, or visual markers) to guide the attention of vision-language models toward specific regions (Shtedritski et al., 2023; Yang et al., 2024). In robotics, this idea has proven effective for injecting high-level priors into control through explicit visual cues. Methods such as RoboGround (Huang

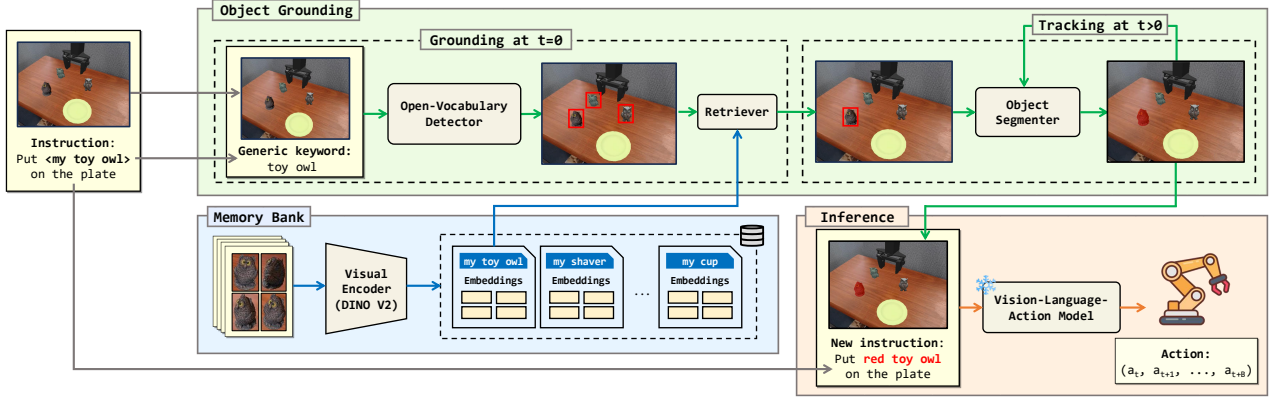


Figure 3. VAP builds a memory from a few reference images and grounds the target object with frozen detection and segmentation modules. It then highlights that object and rewrites the instruction for a frozen VLA, tracking it over subsequent frames and enabling training-free personalized actions.

et al., 2025), MOKA (Liu et al., 2024a), PIVOT (Nasiriany et al., 2024), and TraceVLA (Zheng et al., 2024) leverage visual prompts to improve control or reasoning, whereas we use reference images to resolve user-specific object references, i.e., to select the correct object among lookalikes (e.g., “my cup”). Concretely, we ground the user’s object from a few reference images and highlight it in pixel space, enabling a frozen VLA to reuse its generic manipulation skills while acting on the correct personal instance without per-object fine-tuning.

3. Visual Attentive Prompting

We propose a simple and effective method, Visual Attentive Prompting (VAP), to enable VLA models to manipulate personal objects.

3.1. Problem Formulation

We consider a standard VLA policy $\pi_{\text{VLA}}(a \mid x, \ell)$ that maps an observation x and a language instruction ℓ to an action a . The observation $x = (I, s)$ consists of RGB images $I = \{I^{(v)}\}_{v=1}^V$ from V cameras and the robot’s proprioceptive state s . In our setting, the user provides a small reference set $R_o = \{I_o^{(k)}\}_{k=1}^K$ (where $K \approx 5$) capturing a specific *instance* o that is unseen during training, while its coarse category (e.g., a cup) may be seen. At inference time, the robot confronts a scene containing the target instance alongside visually similar distractors. Our goal is to generate a modified observation \tilde{x} and instruction $\tilde{\ell}$ that enable the frozen π_{VLA} to identify and manipulate the specific target o using only the reference set R_o , without any additional training.

3.2. Overview of VAP

VAP acts as an input-side perceptual adapter: it leaves the VLA parameters untouched and only preprocesses the vi-

sual and language inputs. Instead of changing the policy, it modifies what the model sees and how the instruction is phrased. In this way, a generic manipulation policy can behave as if it understood personalized commands. Intuitively, VAP first decides which pixels correspond to the user’s object in the scene, then reshapes the visual and language inputs so that this region becomes the natural focus of the policy.

Formally, at timestep t the robot receives its usual observation $x_t = (I_t, s_t)$ and a language instruction ℓ , and it is given a small reference set R_o that shows the user’s object o from a few viewpoints. VAP uses these references to construct a prompted observation \tilde{x}_t and instruction $\tilde{\ell}$ that direct the frozen VLA π_{VLA} toward the correct object. We describe this process with a tracking-aware grounding function g and a prompting function p :

$$M_t = g(I_t, R_o, \mathcal{H}_{t-1}), \quad (\tilde{x}_t, \tilde{\ell}) = p(x_t, \ell, M_t)$$

where g initializes M_0 from (I_0, R_o) and propagates it for $t > 0$ using tracking history \mathcal{H}_{t-1} . The mask M_t marks the pixels belonging to the personal object in the current images, and the prompting function p turns this mask into the prompted inputs $(\tilde{x}_t, \tilde{\ell})$. The frozen VLA then simply acts on $(\tilde{x}_t, \tilde{\ell})$, so personalization is handled entirely by g and p operating on its inputs.

To ground the user’s intent in the current scene, VAP treats the reference set R_o as a non-parametric visual memory of the personal object. At execution time, it compares this memory to the live images I_t and selects the pixels that best match the user’s object, producing a mask M_t in each camera view. This mapping turns a personalized reference such as “my cup” into a concrete region in image space.

Once the object is localized, VAP uses the grounded mask to steer the VLA’s attention. It modifies the observation by overlaying a semi-transparent highlight on the masked region and leaving the rest of the scene unchanged, and it

Table 1. Overview of our personalization benchmarks. We report the robot platform, task types, number of tasks and episodes, number of personal object categories, and camera views.

Benchmark	Robot	Task types	#Tasks	#Episodes	#Personal categories	#Cameras
Personalized-SIMPLER (Fractal)	Google Robot	Pick / Move-near	2	1685	2	1
Personalized-SIMPLER (Bridge)	WidowX	Pick / Place	4	96	4	1
Personalized-VLABench	Franka	Selection	5	250	5	3
Real-world	SO-101	Selection / Pick&Place	8	160	8	3

rewrites the instruction into a generic referring expression that matches this visual cue (e.g., from “pick up my cup” to “pick up the red cup”). The policy π_{VLA} then acts on $(\tilde{x}_t, \tilde{\ell})$ as in a standard generic task, but its attention is guided toward the correct instance through the visual prompt, enabling personalized manipulation without any additional training.

3.3. Grounding and Prompting Details

We next describe how the grounding function g and prompting function p are instantiated in practice. Our design uses a coarse-to-fine perception pipeline that identifies the user’s object across time and multiple camera views.

Grounding. We keep a memory \mathcal{M} of user-specific objects. Offline, the user provides a small set of reference images for each personal item. A frozen visual encoder $f(\cdot)$ embeds each reference view $I_o^{(k)}$ of object o , producing vectors $Z_o = \{f(I_o^{(k)})\}_{k=1}^K$. At run time, we load Z_o for the requested object and use embeddings to distinguish the target from generic instances of the same category.

At the start of an episode, we parse the personalized instruction (e.g., “bring my cup”) and extract the generic category name c (“cup”). We use c as a text query for an open-vocabulary detector and run it on each camera view $I_t^{(v)}$. We obtain a set of category-level bounding box proposals $B_t^{(v)} = \{b_i\}_{i=1}^{N_v}$ for view v . This stage finds plausible instances of the category, and personalization happens in the following matching step.

Given the proposals $B_t^{(v)}$ and the reference embeddings Z_o , we retrieve the box that best matches the user’s object. For each candidate $b_i \in B_t^{(v)}$, we crop $I_t^{(v)}[b_i]$, embed it with $f(\cdot)$ to obtain e_i , and compute cosine similarities $\cos(e_i, z_k)$ for all $z_k \in Z_o$. To aggregate evidence across reference views, we ensemble per-reference matches to select the target box:

$$b^* = \operatorname{argmax}_{b_i \in B_t^{(v)}} \sum_{k=1}^K \mathbb{1} \left[i = \operatorname{argmax}_j \cos(e_j, z_k) \right].$$

Each reference view k votes for its most similar proposal, and we select the proposal with the largest vote count, filtering distractors that match the target from the view v .

Once we choose b^* for view v , we refine it into a pixel-wise mask $M_t^{(v)}$ using a class-agnostic segmenter, which yields the per-view masks required by g . For later timesteps ($t > 0$), we avoid rerunning detection and retrieval at every control step. Instead, we apply a real-time tracker that conditions on the current image $I_t^{(v)}$ together with its memory state \mathcal{H}_{t-1} , producing an updated mask $M_t^{(v)}$ and updating the memory online to follow the object as it moves.

Visual Prompting. The masks $\{M_t^{(v)}\}_{v=1}^V$ then instantiate the prompting function p . For each view v , we generate a highlighted image $\tilde{I}_t^{(v)}$ by overlaying a semi-transparent tint on $M_t^{(v)}$ and leaving the background unchanged, and we pass the proprioceptive state s_t through unchanged. At the language level, we rewrite the original instruction ℓ by replacing the personalized span (such as “my cup”) with a generic phrase that matches the visual highlight (such as “the red cup”). We simply apply a template-based rewrite by string matching “my X” and replacing it with “the tint-color X” (e.g., “the red cup”). The frozen VLA is evaluated on $(\{\tilde{I}_t^{(v)}\}_{v=1}^V, s_t, \tilde{\ell})$, which realizes the visual attentive prompting described in Section 3.2 while keeping the underlying policy training-free.

4. Benchmarks

We evaluate VAP on a suite of simulation and real-world benchmarks that instantiate the personalization setting introduced in Figure 2. These benchmarks ask a frozen VLA to act on a user-specific object instance, given a few reference images with same-category distractors. Table 1 summarizes basic statistics.

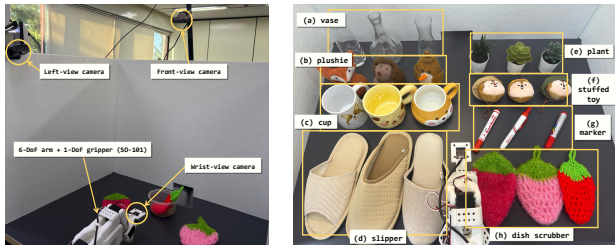
4.1. Simulation Benchmarks

Existing VLA benchmarks mainly test generalization to novel categories or compositional instructions, and seldom require disambiguating a user-designated instance from visually similar distractors using reference images. To study this personalization setting in simulation, we construct *Personalized-SIMPLER* and *Personalized-VLABench* by adapting SIMPLER (Li et al., 2024a) and VLABench (Zhang et al., 2025). In both benchmarks, we preserve the original task semantics but replace one task-relevant object with a user-specific instance, add same-

category distractors, and provide a small reference set R_o for that object. Personalized-SIMPLER focuses on manipulation across two robot embodiments, and Personalized-VLABench isolates multi-view personalized selection, (i.e., the end-effector moves to and touches the personal object). Examples are shown in Figure 2 (top).

Personalized-SIMPLER. SIMPLER provides high-fidelity manipulation environments on common robot platforms (Li et al., 2024a). We personalize six tasks across two single-camera settings: *Fractal* with the Google Robot and *Bridge* with the WidowX arm, where in each episode one task-relevant object is replaced by a personal object and accompanied by same-category distractors. Personal objects are instantiated with 3D assets from Sketchfab,¹ and for each we use five user-provided reference images to form R_o . We follow the original SIMPLER evaluation configurations for both Fractal and Bridge. For Fractal, the visual-matching and variant-aggregation tracks differ only in visual perturbations (lighting, camera pose, background), and systematically enumerating these variants yields 1,685 personalized episodes. For Bridge, the original SIMPLER configuration provides 96 evaluation episodes (Table 1).

Personalized-VLABench. VLABench is a large-scale benchmark for language-conditioned manipulation and long-horizon reasoning (Zhang et al., 2025). We adapt it to five selection-style tasks on a Franka arm with three synchronized cameras. Each task defines a personal category (bags, shoes, figurines, miniatures, tableware); in each episode, one object in the scene is replaced by a user-specific instance and two same-category distractors are added. As in Personalized-SIMPLER, we use 3D models from Sketchfab and use 5 user-provided reference images of each personal object to form R_o . Episodes provide the personalized instruction (e.g., “select my leather bag”), the reference images, and the three camera views. Personalized-VLABench contains 5 tasks with 50 episodes each.



(a) The real-world hardware setup, featuring the SO-101 robot arm and a consists of one target personal object multi-view camera system. (b) Objects used in the real-world experiments. Each of the 8 categories and two distractors.

Figure 4. Overview of our real-world experimental setup.

¹<https://sketchfab.com>

4.2. Real-world Benchmarks

In addition to simulation, we construct a real-world personalization benchmark that follows the same structure. The physical setup is shown in Figure 4, and example tasks are visualized in Figure 2 (bottom).

Our setup consists of a tabletop workspace, a 6-DoF SO-101 robot arm² with a 1-DoF parallel gripper, and three RGB cameras (front, side, and wrist). We consider eight everyday categories: vase, plushie, cup, slipper, plant, stuffed toy, marker, and dish scrubber. For each category, we collect three *unseen* physical instances from local stores and office environments. One is designated as the personal object and two serve as visually similar distractors.

Each episode places the three instances of a category and provides a small set of reference images of the personal object, captured from the real cameras and cropped to form R_o , together with a personalized instruction (e.g., “select my slipper” or “put my scrubber into the plastic bowl”). We include both selection and pick-and-place tasks, yielding a real-world benchmark that evaluates whether a policy adapted via VAP can reliably identify and manipulate user-specific objects on physical hardware.

5. Experiments

We now describe the experimental setup, baselines, and metrics used to evaluate VAP on the benchmarks in Section 4. Additional experimental details, including environment configurations and hyperparameters, are provided in Appendix A.

5.1. Experimental Setup

We evaluate VAP in both simulation and real-world settings to assess how well it personalizes a pre-trained VLA to user-specific objects.

Backbone VLA. Unless otherwise stated, we use $\pi_{0.5}$ (Intelligence et al., 2025) as the backbone VLA policy. For experiments on Personalized-SIMPLER, we instead use the π_0 checkpoint released for the Fractal and Bridge settings in the open-source repository,³ following prior work showing that π_0 attains consistently strong performance on these settings (Fang et al., 2025). We fine-tune $\pi_{0.5}$ solely for environment adaptation on generic data that excludes personal objects and personalized instructions, and then keep the backbone frozen for VAP and all baselines. In all experiments, the chosen backbone VLA is used as provided and remains frozen; VAP and all baselines share the same

²<https://huggingface.co/docs/lerobot/sol101>

³<https://github.com/allenzren/open-pi-zero>

Table 2. Performance on the **Personalized-SIMPLER** benchmark with the **Google-Robot** platform. VAP consistently outperforms all baselines. The two tracks evaluate matching against single objects and aggregates of visually similar objects.

Method	Task 1: Pick my pen holder		Task 2: Move my bottle near coke can	
	CMR (%)	SR (%)	CMR (%)	SR (%)
<i>Track 1: Visual Matching with Unseen Personalization Objects</i>				
π_0	10.5	8.5	50.4	48.6
π_0 + Soft Prompt	33.1	24.0	60.0	51.7
π_0 + Hard Prompt (Short)	11.0	8.9	66.7	57.5
π_0 + Hard Prompt (Long)	11.2	9.1	64.5	58.8
π_0 + VAP	89.2	60.3	73.2	60.6
<i>Track 2: Variant Aggregation with Unseen Personalization Objects</i>				
π_0	17.4	10.2	49.2	41.3
π_0 + Soft Prompt	31.8	26.4	57.7	44.7
π_0 + Hard Prompt (Short)	21.6	14.4	71.5	54.2
π_0 + Hard Prompt (Long)	17.3	12.6	67.7	51.3
π_0 + VAP	87.3	58.2	72.4	58.2

Table 3. Performance on the **Personalized-SIMPLER** benchmark using the **WidowX** platform across four manipulation tasks. For each task, we evaluate 10 runs of 24 episodes. VAP’s modular perception pipeline achieves consistently high success rates, whereas prior methods struggle to personalize.

Method	Task 3: Pick shaver		Task 4: Put camera		Task 5: Put owl		Task 6: Put straw cup	
	CMR (%)	SR (%)	CMR (%)	SR (%)	CMR (%)	SR (%)	CMR (%)	SR (%)
π_0	0.0	0.0	34.2	31.7	35.2	30.3	80.6	27.8
π_0 + Soft Prompt	25.0	8.3	54.2	41.7	79.2	62.5	87.5	29.2
π_0 + Hard Prompt (Short)	0.0	0.0	50.0	25.0	37.5	33.3	83.3	29.2
π_0 + Hard Prompt (Long)	0.0	0.0	53.2	27.9	36.0	31.6	83.4	30.1
π_0 + VAP	82.9	71.3	92.1	92.1	100.0	95.0	100.0	75.6

Table 4. Success Rates (%) on the **Personalized-VLAbench** benchmark. For each task, we evaluate 10 runs of 25 episodes. VAP outperforms other baselines across all scenarios.

Method	Task 1: Leather bag	Task 2: Shoe	Task 3: Cat figurine	Task 4: Miniature house	Task 5: Cup
$\pi_{0.5}$	33.6	30.4	35.2	29.6	40.4
$\pi_{0.5}$ + Soft Prompt	51.2	40.8	44.4	39.6	54.8
$\pi_{0.5}$ + Hard Prompt (Short)	52.4	37.6	44.0	38.8	51.6
$\pi_{0.5}$ + Hard Prompt (Long)	52.0	39.6	42.8	39.6	50.0
$\pi_{0.5}$ + VAP	89.2	54.0	51.6	52.4	60.8

backbone in each setting. Further details on the training and adaptation of π_{VLA} are given in Appendix A.2.

Evaluation Metrics. We report Success Rate (SR), the fraction of episodes that complete the task, following standard VLA evaluations (Intelligence et al., 2025; Kim et al., 2024). For pick and pick-and-place tasks, we also report Correct Movement Ratio (CMR), the fraction of episodes that move the correct personal object at least once, regardless of final success (Sridhar et al., 2025). CMR is not defined for pointing or selection tasks. Higher values are better for all metrics.

Implementation. For the input-side module in VAP, we use DINOv2 (Oquab et al., 2023) as the visual encoder, Grounding DINO (Liu et al., 2024b) as the open-vocabulary detector, and SAM2 (Ravi et al., 2024) for segmentation and tracking.

5.2. Baselines

We evaluate the following methods, all using the same VLA backbone in each setting.

- **Generic VLA:** A naive baseline that uses VLA alone, feeding the personalized instruction directly to the model (e.g., “pick up my shaver”) and measuring its behavior without any personalization mechanism.
- **Hard Prompt (Short/Long):** A language-based baseline that rewrites the personalized instruction with an LLM into a short or long generic description conditioned on a textual description of the object derived from its reference images. The resulting description is prepended to the instruction at inference time (see Appendix A.3 for details).
- **Soft Prompt (Token Learning):** A token-learning baseline adapted from prior VLM personalization method Yo’LLaVA (Nguyen et al., 2024). For each personal object, we learn single token embedding in the underlying VLM from its reference images and then copy these learned embeddings into the VLA’s language embedding space. At inference time, the learned tokens are prepended to the instruction while keeping all VLA parameters fixed.

To ensure a strong Soft Prompt baseline, we train it with Yo’LLaVA-style supervision, achieving > 95% accuracy on a VQA-style recognition task, and by using oracle hard negatives drawn from test-time objects. We further confirm that the learned concept token transfers into the VLA with small embedding shift and yields object-centric spatial attention (Appendix B). Nevertheless, end-to-end manipulation improvements remain limited (Section 5.3, 5.4).

5.3. Results on Simulation Benchmarks

We first study how VAP affects instance-level manipulation in the simulation benchmarks. Tables 2, 3, and 4 report SR and CMR for Personalized-SIMPLER and SR for Personalized-VLABench.

On **Personalized-SIMPLER** (Google Robot), VAP substantially improves both correct-object interaction (CMR) and task completion (SR), with the largest gains on the pen-holder task where the generic π_0 and language-based baselines frequently pick up distractors. In the visual-matching track, VAP increases SR from 8.5% to 60.3% and CMR from 10.5% to 89.2%, showing that the policy interacts with the correct instance much more reliably once the visual prompt is provided. Under variant aggregation, VAP still maintains similar performance (SR 58.2%, CMR 87.3%). On the bottle task, language-only hard prompts perform competitively, likely because the required manipulation is less demanding than in the pen-holder tasks, while VAP remains consistently strong.

The WidowX setting reveals an even sharper separation between VAP and baselines. In the task 3, the generic policy and hard prompts rarely manipulate the correct object, and soft prompts achieve only limited success, whereas VAP reaches CMR/SR of 82.9/71.3. A similar pattern appears in the placement tasks: soft prompts can achieve high CMR yet fail to convert that interaction into task completion. For example, on Task 5, Soft Prompt attains CMR 79.2% with SR 62.5%, while VAP achieves 100.0% CMR and 95.0% SR. The gap is larger on Task 6, where Soft Prompt reaches CMR 87.5% but SR only 29.2% (vs. 100.0/75.6 with VAP). While the high CMR may partly reflect incidental object motion in a tightly cluttered setting, VAP still achieves much higher SR, showing more reliable end-to-end task completion.

Personalized-VLABench evaluates multi-view personalized selection with the $\pi_{0.5}$ backbone (Table 4). Text-based prompting yields consistent improvements over the generic policy across all categories. For example, on leather bag SR increases from 33.6% to 51.2–52.4% with Soft/Hard prompts thanks to stronger VLA backbones. Nevertheless, VAP achieves the best SR on all five object categories, with the largest margin on leather bag (+36.8 points over the best prompt baseline) and consistent gains on other categories.

Across benchmarks, Soft Prompt exhibits a recurring pattern. It can bias the policy toward the correct instance and yield moderate gains in CMR, but these gains do not reliably translate into end-to-end task completion (SR), particularly on placement tasks. We provide additional details and analysis of the token-learning baseline in Appendix B and Appendix B.3.

Phase	Component	Time (s)
Init. (1st frame)	Grounding DINO	0.19
	Crop / embed / segment	0.07
Per step	SAM2 tracking	0.02
	VLA policy inference	0.20

Table 5. Average runtime of the components of VAP in Personalized-SIMPLER. The initialization phase runs once at the beginning of each episode, while SAM2 tracking and VLA policy inference are executed at every control step.

5.4. Results on Real-world Benchmark

We next evaluate VAP on the real-world benchmark, which consists of four pointing tasks and four pick-and-place tasks executed with the $\pi_{0.5}$ policy. Figure 5 reports Success Rate (SR) for all tasks and Correct Movement Ratio (CMR) for pick-and-place.

On average across the four pointing tasks, VAP raises SR from 30.0% for the generic $\pi_{0.5}$ to 80.0%, while language-based hard and soft prompts reach 40.0–45.0%. These results suggest that text-only method remains prone to same-category distractors, whereas pixel-space prompting helps disambiguate the user’s specific instance.

The same trend holds for pick-and-place tasks, which require longer-horizon control. Averaged over the four pick-and-place tasks, SR increases from 18.8% for $\pi_{0.5}$ to 56.2% with VAP, while hard and soft prompts remain in the 26.2–30.0% range. CMR further shows that text- and token-based baselines can sometimes move the correct object at least once but still fail to complete the placement, leading to a larger CMR–SR gap. In contrast, VAP achieves higher SR together with high CMR, indicating more consistent end-to-end completion in real-world execution.

	Personalized-SIMPLER (Fractal)	Personalized-SIMPLER (Bridge)	Personalized-VLABench	Real-world Scenarios
Fail (%)	37.6	16.6	38.4	31.9
Case 1 (%)	13.1	21.4	—	—
Case 2 (%)	—	—	59.2	50.9
Case 3 (%)	86.9	78.6	40.8	49.1

Table 6. Error-case of VAP across benchmarks. Fail is overall and Case 1–3 are conditional on failure and — denotes not applicable.

5.5. Error Case Analysis

While VAP consistently improves performance, it still exhibits a few recurring failure patterns across Personalized-SIMPLER, Personalized-VLABench, and our real-world benchmark. As summarized in Table 6, single-view settings are rarely limited by prompt ambiguity (Case 1 accounts for only 13.1%/21.4% of failures in Fractal/Bridge), and most failures occur even with correct prompting, indicating that manipulation difficulty dominates in these regimes. In contrast, multi-view settings are primarily af-

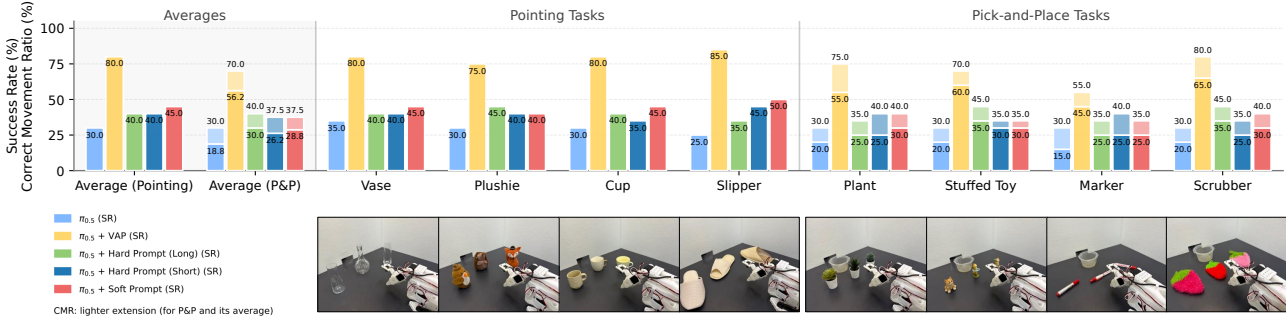


Figure 5. Performance on real-world tasks, averaged over 20 trials. We report Success Rate (SR) for all tasks and Correct Movement Ratio (CMR) for pick-and-place tasks. The CMR metric is not applicable for pointing tasks. VAP demonstrates a consistently high success rate across all scenarios, consistently outperforming the baseline.

ected by cross-view inconsistency (Case 2 accounts for 59.2% and 50.9% of failures in Personalized-VLABench and Real-world), where the personal object is not visible in a subset of cameras and grounding/tracking can drift—most notably under occlusion in the side view. We provide qualitative examples and further discussion of these multi-view and control-related failure modes in Appendix D.

5.6. Efficiency of VAP

A natural concern with VAP is whether the additional perception modules incur prohibitive runtime overhead compared to running the frozen VLA alone. Table 5 summarizes the average component runtimes in our Personalized-SIMPLER implementation. At the start of each episode, VAP establishes the personalized mask with a one-time initialization cost of 0.26 s, consisting of Grounding DINO for category proposal generation (0.19 s) plus cropping, feature embedding, and initial segmentation (0.07 s). During control, the dominant cost remains VLA inference at 0.20 s per step, while SAM2 performs mask tracking in 0.02 s per frame, adding only a 10% overhead per step. Overall, VAP adds modest wall-clock cost beyond the base policy while enabling the substantial improvements in SR and CMR reported in Sections 5.3 and 5.4.

6. Conclusion

We introduce Visual Attentive Prompting (VAP), a simple-yet-effective training-free personalization pipeline that enables frozen VLA models to manipulate user-specific objects from a few reference images by grounding the target and prompting the policy with a mask-based highlight aligned with an instruction rewrite. Across two simulation benchmarks and a real robot, VAP improves success and correct-object interaction over personalization baselines. At the same time, VAP still depends on the quality of the initial segmentation and on maintaining consistent masks across camera views, and we evaluate primarily single-object, short-horizon tasks. We therefore view

our work as a core building block for richer forms of personalization, such as user-specific spatial conventions (e.g., “my side of the desk”) and personalized multi-step routines, whose robustness under more challenging real-world conditions we leave for future work.

References

Alaluf, Y., Richardson, E., Tulyakov, S., Aberman, K., and Cohen-Or, D. Myvlm: Personalizing vlms for user-specific queries, 2024.

Barsellotti, L., Bigazzi, R., Cornia, M., Baraldi, L., and Cucchiara, R. Personalized instance-based navigation toward user-specific objects in realistic environments. *Advances in Neural Information Processing Systems*, 37: 11228–11250, 2024.

Beyer, L., Steiner, A., Pinto, A. S., Kolesnikov, A., Wang, X., Salz, D., Neumann, M., Alabdulmohsin, I., Tschanen, M., Bugliarello, E., et al. Paligemma: A versatile 3b vlm for transfer. *arXiv preprint arXiv:2407.07726*, 2024.

Black, K., Brown, N., Driess, D., Esmail, A., Equi, M., Finn, C., Fusai, N., Groom, L., Hausman, K., Ichter, B., Jakubczak, S., Jones, T., Ke, L., Levine, S., Li-Bell, A., Mothukuri, M., Nair, S., Pertsch, K., Shi, L. X., Tanner, J., Vuong, Q., Walling, A., Wang, H., and Zhilinsky, U. π_0 : A vision-language-action flow model for general robot control. *arXiv preprint arXiv:2410.24164*, 2024.

Brohan, A., Brown, N., et al. Rt-2: Vision-language-action models transfer web knowledge to robotic control. *arXiv preprint arXiv:2307.15818*, 2023.

Fang, H.-S., Fang, H., et al. Rh20t: A comprehensive robotic dataset for learning diverse skills in one-shot. In *Proceedings of Robotics: Science and Systems (RSS)*, 2023.

- Fang, I., Zhang, J., Tong, S., and Feng, C. From intention to execution: Probing the generalization boundaries of vision-language-action models. *arXiv preprint arXiv:2506.09930*, 2025.
- Fu, Y., Wang, R., Ren, B., Sun, G., Gong, B., Fu, Y., Paudel, D. P., Huang, X., and Van Gool, L. Objectre-ator: Enabling cross-view object relation understanding across ego-centric and exo-centric perspectives. In *Proceedings of the IEEE/CVF International Conference on Computer Vision*, pp. 6530–6540, 2025.
- Gal, R., Alaluf, Y., Atzmon, Y., Patashnik, O., Bermano, A. H., Chechik, G., and Cohen-Or, D. An image is worth one word: Personalizing text-to-image generation using textual inversion. In *Advances in Neural Information Processing Systems*, volume 35, pp. 30309–30322, 2022.
- Grannen, J., Karamcheti, S., Wulfe, B., and Sadigh, D. Provox: Personalization and proactive planning for situated human-robot collaboration. *IEEE Robotics and Automation Letters (RA-L)*, 2025.
- Hao, Y., Dong, L., Wei, F., and Xu, K. Investigating learning dynamics of bert fine-tuning. In *Proceedings of the 1st conference of the Asia-Pacific Chapter of the Association for Computational Linguistics and the 10th international joint conference on natural language processing*, pp. 87–92, 2020.
- Huang, H., Chen, X., Chen, Y., Li, H., Han, X., Wang, Z., Wang, T., Pang, J., and Zhao, Z. Roboground: Robotic manipulation with grounded vision-language priors. In *Proceedings of the Computer Vision and Pattern Recognition Conference*, pp. 22540–22550, 2025.
- Intelligence, P., Black, K., Brown, N., Darpinian, J., Dhabalia, K., Driess, D., Esmail, A., Equi, M., Finn, C., Fusaï, N., Groom, L., Hausman, K., Ichter, B., et al. $\pi_{0.5}$: A vision-language-action model with open-world generalization. *arXiv preprint arXiv:2504.16054*, 2025.
- Kawaharazuka, K., Oh, J., Yamada, J., Posner, I., and Zhu, Y. Vision-language-action models for robotics: A review towards real-world applications. *IEEE Access*, 13: 162467–162504, 2025. doi: 10.1109/ACCESS.2025.3609980.
- Khazatsky, A., Pertsch, K., Nair, S., Balakrishna, A., et al. Droid: A large-scale in-the-wild robot manipulation dataset. In *Proceedings of Robotics: Science and Systems (RSS)*, 2024.
- Kim, M. J., Pertsch, K., Karamcheti, S., Xiao, T., Balakrishna, A., Nair, S., Rafailov, R., Foster, E., Lam, G., San- keti, P., Vuong, Q., Kollar, T., Burchfiel, B., Tedrake, R., Sadigh, D., Levine, S., Liang, P., and Finn, C. Openvla: An open-source vision-language-action model. *arXiv preprint arXiv:2406.09246*, 2024.
- Kumari, N., Zhang, B., Wang, R., Shechtman, E., Zhang, R., and Zhu, J.-Y. Multi-concept customization of text-to-image diffusion. In *Proceedings of the IEEE/CVF Conference on Computer Vision and Pattern Recognition (CVPR)*, pp. 1931–1941, 2023.
- Kwon, T., Choi, D., Kim, S., Kim, H., Moon, S., Kwak, B.-w., Huang, K.-H., and Yeo, J. Embodied agents meet personalization: Investigating challenges and solutions through the lens of memory utilization. *arXiv preprint arXiv:2505.16348*, 2025.
- Li, X., Hsu, K., Gu, J., Pertsch, K., Mees, O., Walke, H. R., Fu, C., Lunawat, I., Sieh, I., Kirmani, S., et al. Evaluating real-world robot manipulation policies in simulation. *arXiv preprint arXiv:2405.05941*, 2024a.
- Li, Z., Cao, M., Wang, X., Qi, Z., Cheng, M.-M., and Shan, Y. Photomaker: Customizing realistic human photos via stacked id embedding. In *Proceedings of the IEEE/CVF Conference on Computer Vision and Pattern Recognition (CVPR)*, pp. 8609–8619, 2024b.
- Liu, F., Fang, K., Abbeel, P., and Levine, S. Moka: Open-world robotic manipulation through mark-based visual prompting. In *Proceedings of Robotics: Science and Systems (RSS)*, 2024a.
- Liu, S., Zeng, Z., Ren, T., Li, F., Li, J., Ren, H., Zhang, Z., Yang, J., Su, H., Zhu, J., and Zhang, L. Grounding dino: Marrying dino with grounded pre-training for open-set object detection. In *Proceedings of the European Conference on Computer Vision*, 2024b.
- Merchant, A., Rahimtoroghi, E., Pavlick, E., and Tenney, I. What happens to bert embeddings during fine-tuning? *arXiv preprint arXiv:2004.14448*, 2020.
- Nasiriany, S. et al. Pivot: Iterative visual prompting elicits actionable knowledge for vlms. In *Conference on Robot Learning (CoRL)*, 2024.
- Nguyen, T., Liu, H., Li, Y., Cai, M., Ojha, U., and Lee, Y. J. Yo’llava: Your personalized language and vision assistant, 2024. URL <https://arxiv.org/abs/2406.09400>.
- NVIDIA. Gr00t n1.5: An improved open foundation model for generalist humanoid robots, 2025. URL https://research.nvidia.com/labs/gear/gr00t-n1_5/.
- Octo Model Team, Chitnis, R., et al. Octo: An open-source general-purpose robot manipulation policy. In *Proceedings of Robotics: Science and Systems (RSS)*, 2024.

- O’Neill, A., Rehman, A., and Collaboration, O. X.-E. Open x-embodiment: Robotic learning datasets and rt-x models. *arXiv preprint arXiv:2310.08864*, 2023.
- Oquab, M., Darcet, T., Mazare, P., and Bojanowski, P. Dinov2: Learning robust visual features without supervision. *arXiv preprint arXiv:2304.07193*, 2023.
- Physical Intelligence et al. $\pi_{0.6}$: a vla that learns from experience. *Technical Report*, 2025. URL <https://www.physicalintelligence.company/download/pistar06.pdf>.
- Ravi, N., Gabeur, V., Hu, Y.-T., Hu, R., Ryali, C., Ma, T., Khedr, H., Rädle, R., Rolland, C., Gustafson, L., et al. Sam 2: Segment anything in images and videos. *arXiv preprint arXiv:2408.00714*, 2024.
- Ruiz, N., Li, Y., Jampani, V., Pritch, Y., Rubinstein, M., and Aberman, K. Dreambooth: Fine tuning text-to-image diffusion models for subject-driven generation. In *Proceedings of the IEEE/CVF Conference on Computer Vision and Pattern Recognition*, pp. 22500–22510, 2023.
- Shtedritski, A., Rupprecht, C., and Vedaldi, A. What does clip know about a red circle? visual prompt engineering for vlms. In *Proceedings of the IEEE/CVF International Conference on Computer Vision*, 2023.
- Sridhar, K., Dutta, S., Jayaraman, D., and Lee, I. Ricl: Adding in-context adaptability to pre-trained vision-language-action models. *arXiv preprint arXiv:2508.02062*, 2025.
- Tan, Z. et al. Democratizing large language models via personalized parameter-efficient fine-tuning. *arXiv preprint arXiv:2402.14069*, 2024.
- Walke, H., Black, K., Lee, A., Kim, M. J., et al. Bridgedata v2: A dataset for robot learning at scale. In *Conference on Robot Learning (CoRL)*, 2023.
- Wen, J., Zhu, M., Zhu, Y., Tang, Z., Li, J., Zhou, Z., Li, C., Liu, X., Peng, Y., Shen, C., et al. Diffusion-vla: Generalizable and interpretable robot foundation model via self-generated reasoning. *arXiv preprint arXiv:2412.03293*, 2024.
- Wu, J., Antonova, R., Kan, A., Lepert, M., Zeng, A., Song, S., Bohg, Jeannette and BZhimin, S., and Goldstein, T. Tidybot: Personalized robot assistance with large language models. In *International Conference on Intelligent Robots and Systems (IROS)*, 2023.
- Yang, J., Zhang, H., Li, F., Zou, X., Li, C., and Gao, J. Set-of-mark prompting unleashes extraordinary visual grounding in gpt-4v. In *Proceedings of the IEEE/CVF Conference on Computer Vision and Pattern Recognition (CVPR)*, 2024.
- Ye, H., Zhang, J., Liu, S., Han, X., and Yang, W. Ip-adapter: Text compatible image prompt adapter for text-to-image diffusion models. *arXiv preprint arXiv:2308.06721*, 2023.
- Zhang, R., Jiang, Z., Guo, Z., Yan, S., Pan, J., Ma, X., Dong, H., Gao, P., and Li, H. Personalize segment anything model with one shot. In *Proceedings of the International Conference on Learning Representations*, 2024.
- Zhang, S., Xu, Z., Liu, P., Yu, X., Li, Y., Gao, Q., Fei, Z., Yin, Z., Wu, Z., Jiang, Y.-G., et al. Vlabench: A large-scale benchmark for language-conditioned robotics manipulation with long-horizon reasoning tasks. In *Proceedings of the IEEE/CVF International Conference on Computer Vision*, pp. 11142–11152, 2025.
- Zhao, W., Ding, P., Zhang, M., Gong, Z., Bai, S., Zhao, H., and Wang, D. Vlas: Vision-language-action model with speech instructions for customized robot manipulation. *arXiv preprint arXiv:2502.13508*, 2025. ICLR 2025.
- Zheng, R., Liang, Y., Huang, S., Gao, J., Daumé III, H., Kolobov, A., Huang, F., and Yang, J. Tracevla: Visual trace prompting enhances spatial-temporal awareness for generalist robotic policies. *arXiv preprint arXiv:2412.10345*, 2024.
- Zhong, W. et al. Memorybank: Enhancing large language models with long-term memory for personalized applications. In *Proceedings of the AAAI Conference on Artificial Intelligence*, 2024.

A. Experimental Details

A.1. Hardware and Software Settings

All experiments were conducted on a Linux server equipped with an Intel Xeon Gold 6230 CPU @ 2.10 GHz, 1 TB of RAM, and four NVIDIA RTX A6000 GPUs, running Ubuntu 22.04.3 LTS. Unless otherwise specified, VLA inference used a single RTX A6000 GPU. For training the VLA policies used in our experiments, we used four NVIDIA A100 GPUs. Our code is implemented in Python using PyTorch and builds on the public $\pi_0/\pi_{0.5}$ implementation.

A.2. Training VLAs

We use the released checkpoint of π_0 for Personalized-SIMPLER, and train $\pi_{0.5}$ for Personalized-VLABench and the real-world experiments. This subsection describes the dataset construction and training configurations for $\pi_{0.5}$.

Training Dataset for Personalized-VLABench. We base our dataset on the `select_painting` task in VLABench. The original task requires the agent to press a red button corresponding to a target painting, which introduces an extra gap between object localization and motor control. To better match our personalized object manipulation setting, we modify the task so that the agent directly touches the target object on the table instead of pressing a button.

For each episode, we spawn a single painting at a random position on the table and issue the generic instruction “*select the painting*”. We use the RRT-based motion planner provided by VLABench to generate expert trajectories. Rather than directly copying the planner states, we execute the planned waypoints on the robot via inverse kinematics and record the resulting joint states. Given a state sequence $\{s_t\}_{t=0}^T$, we train the policy to predict state deltas $a_t = s_{t+1} - s_t$ instead of absolute states, which we found to yield more stable behavior in downstream control. We generate 500 training episodes with randomized object positions. Figure 6 shows example episodes from the Personalized-VLABench training data.

Training Dataset for Real-world Scenarios. To adapt $\pi_{0.5}$ to the real-world tabletop setting, we collect a small, task-specific dataset using teleoperation on the SO-101 arm. We define five tasks: two selection tasks (“*point at the cup*”, “*point at the cat figurine*”) and three pick-and-place tasks (“*put the miniature house into the plastic bowl*”, “*put the owl figurine into the plastic bowl*”, “*put the red bus into the plastic bowl*”). All training objects in this dataset are disjoint from the personal objects used at evaluation time, so the policy only learns generic selection and pick-and-place skills rather than memorizing specific items.

For each task, we collect 50 teleoperated episodes at 30 Hz using the onboard RGB cameras, resulting in 250 episodes in total. As in the simulation setting, we train the policy to predict joint-space deltas between consecutive states. This dataset allows $\pi_{0.5}$ to adapt to the kinematics, camera viewpoints, and workspace of the real-world setup while keeping the personal objects unseen during training. Figure 7, 8 shows example episodes from the real-world scenario training data.

Training settings. For both Personalized-VLABench and the real-world dataset, we initialize $\pi_{0.5}$ from the public checkpoint and fine-tune it with the same hyperparameters. We use a batch size of 64, an action dimension of 32, and an action horizon of 4, and train for 60,000 gradient steps using Adam. We train on a single node with four A100 GPUs and use the final iteration as the last checkpoint.

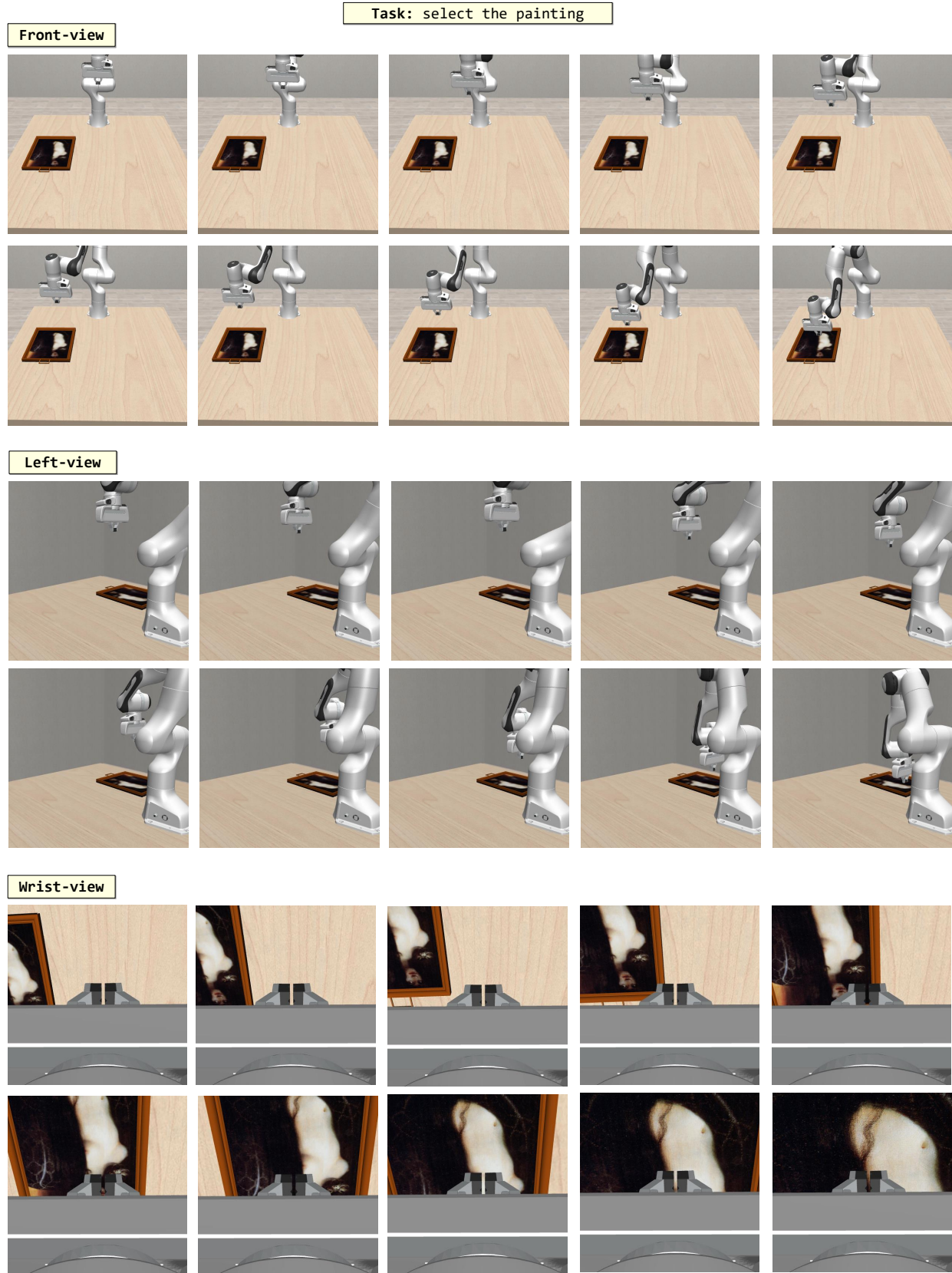


Figure 6. Example training sample for Personalized-VLABench

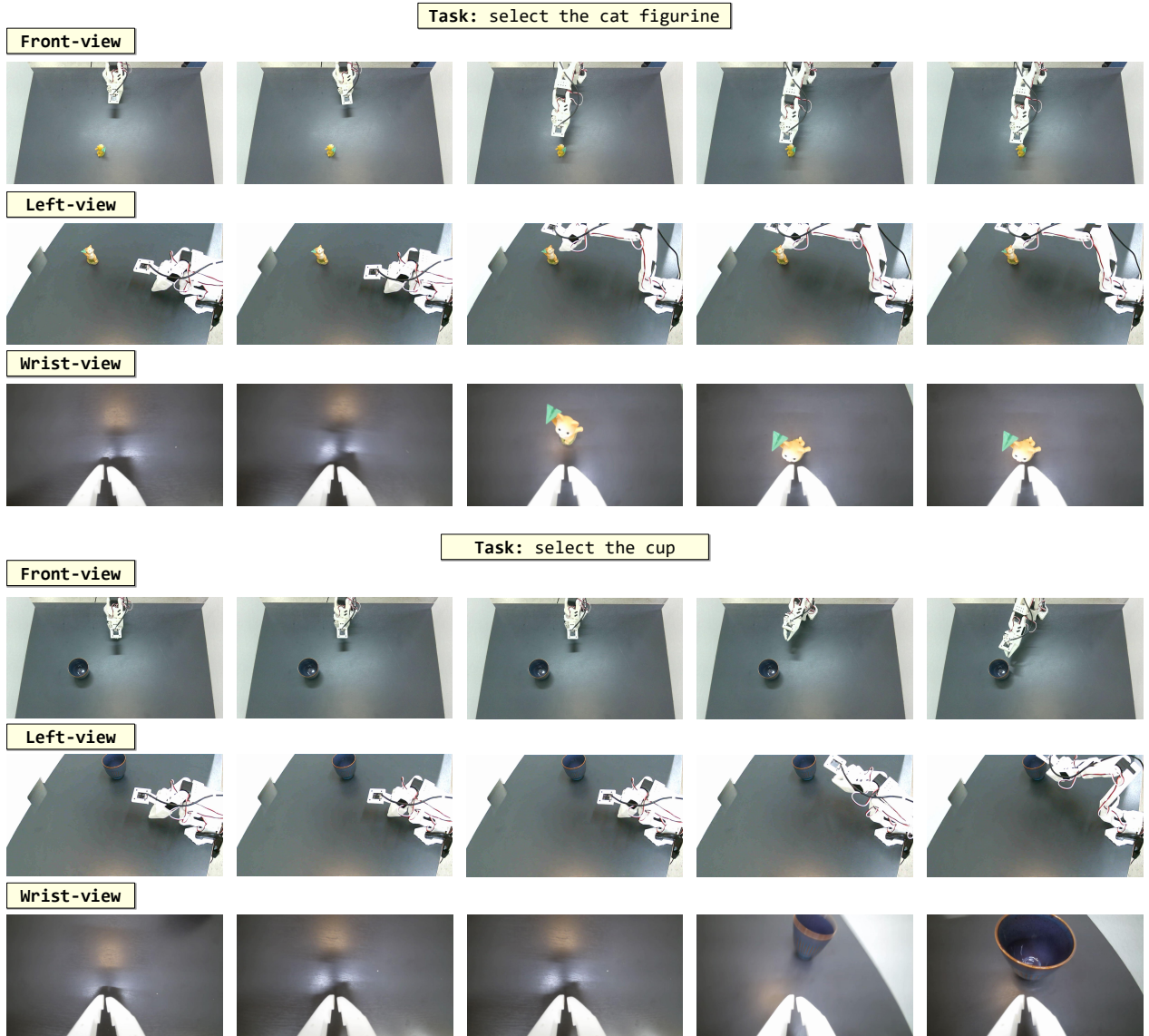


Figure 7. Example training sample for real-world scenarios (selection)

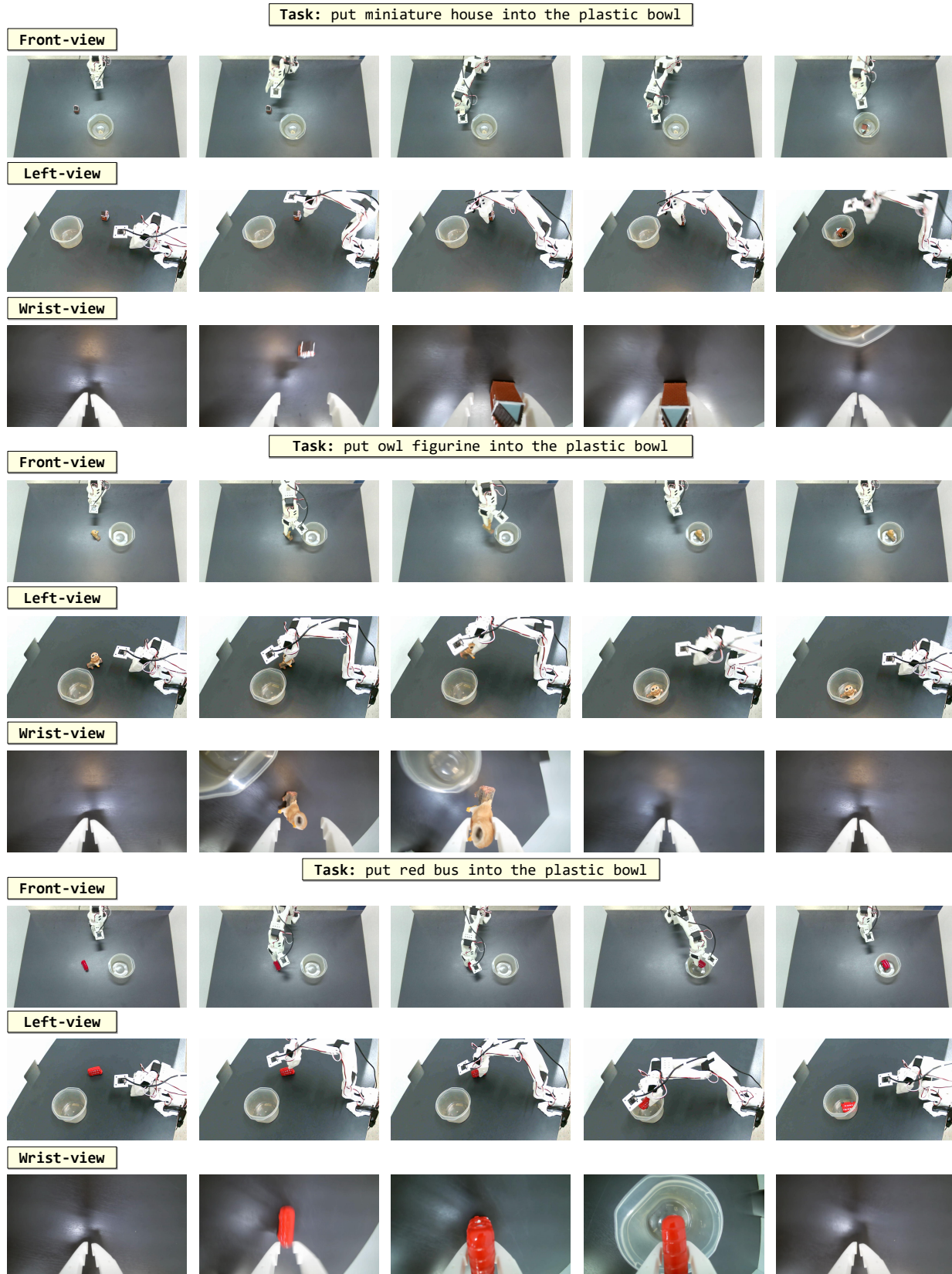


Figure 8. Example training sample for real-world scenarios (pick-and-place)

A.3. Generating Textual Descriptions

We require short and long textual descriptions of each personal object to construct hard and short prompt baselines. To obtain these descriptions, we use GPT-4o with following prompts (for long and short each). For each object, we choose one canonical reference view (front-facing if available) and query the model once.

Prompt Used to Generate Long Textual Description for Hard Prompt Methods

Describe only the object in the image. Focus on its most distinctive features such as shape, color, and material. Write the result in English as a short noun phrase, not a full sentence. Do not mention orientation, position, or surroundings.

Prompt Used to Generate Short Textual Description for Hard Prompt Methods

Describe only the object in the image. Write the result in English as a single, highly detailed noun phrase, not a full sentence. Include as many intrinsic and identifying features as possible, such as overall shape, dimensions, proportions, material, surface finish, textures, patterns, colors, edges, rims, openings, and any decorative or structural details. Do not mention orientation, position, or surroundings.

We manually verify that the generated phrases correctly describe each object and lightly edit obviously incorrect attributes when necessary. We then use the short descriptions as hard prompts and the long descriptions as rich prompts for our personalization baselines. Table 7 in the appendix lists the final short and long descriptions for objects in Personalized-SIMPLER, Personalized-VLABench, and the real-world scenarios.

Table 7. Short and long textual descriptions for personal objects used in our benchmarks. Short descriptions and long descriptions are used as rich prompts for personalization baselines (hard prompt).

Object	Short description	Long description
<i>Personalized-SIMPLER</i>		
pen holder	black cylindrical mesh pen holder	a cylindrical, black metal mesh pen holder with a smooth, solid circular base, featuring a fine grid pattern on the sides, a slightly flared top rim, and a matte finish
bottle	black cylindrical bottle with a red cap	a small, cylindrical black bottle with a smooth matte finish, featuring a colorful label with text and graphics, a slightly rounded cap, and a compact, uniform structure
shaver	a sleek black electric shaver with a curved handle and three rotary blades	a sleek, compact electric shaver with a matte black finish, featuring a slightly curved ergonomic handle for a comfortable grip, a glossy black control panel with subtle button details, and a rounded shaving head with three circular, silver metallic rotary blades encased in a dark gray protective mesh
camera	a small, black, cylindrical camera with a glossy finish	a small, black, rectangular camera with a cylindrical lens protruding from the front, featuring a glossy finish, smooth surfaces, subtle horizontal grooves on the body, a silver ring around the lens, and a small, circular button on the top

continued on next page

Object	Short description	Long description
owl figurine	small, dark, textured owl ornament	a small, intricately carved owl figurine with a rounded body and prominent, detailed facial features, crafted from a dark, glossy material with subtle metallic sheen, featuring textured feather patterns across its surface, large circular eyes with a reflective finish, and a smooth, flat base for stability
straw cup	pink and white striped cup with a gray straw	a cylindrical cup with a tapered base, featuring a smooth surface adorned with alternating pink and white diagonal stripes, topped with a flat, circular lid with a central opening for a slender, straight, gray straw

Personalized-VLABench

leather bag	dark brown leather briefcase with a buckle clasp	a compact, rectangular, dark brown leather briefcase with a smooth surface finish, featuring a single flap closure secured by a metal clasp, a sturdy handle attached to the top, and subtle stitching along the edges for reinforcement
shoe	blue and gray athletic shoe with black laces and a chunky sole	a sleek athletic shoe with a rounded toe, featuring a combination of blue and gray synthetic materials, a mesh upper for breathability, a cushioned collar and tongue, a lace-up closure with black laces, a textured rubber outsole for traction, and subtle decorative stitching along the sides
cat figurine	small black plush cat	a small, sleek black cat with a glossy coat, compact body, rounded ears, and a curled tail
miniature house	red and green toy house with a flat roof	a small, rectangular, toy-like house with a red roof, red walls, and blue windows, featuring a green base and a simple, blocky design
cup	a dark brown, cylindrical paper cup	a cylindrical, dark brown paper cup with a smooth matte finish, medium height, slightly tapered sides, a thin rolled rim, and an open top

Real-world scenarios

vase	clear glass vase with a narrow neck and bulbous base	a clear glass vase with a tall, narrow neck and a wide, bulbous base, featuring a smooth, glossy surface with subtle vertical ridges, a slightly flared rim, and a transparent finish that reveals the intricate reflections and refractions within
-------------	--	---

continued on next page

Object	Short description	Long description
plushie	brown and pink fuzzy hedgehog plushie with a round body and pointed snout	a round, fuzzy plushie resembling a hedgehog with a soft, felt-like texture, featuring a light brown body and a darker brown, fluffy mane encircling its back, a protruding snout with a small, rounded brown nose, tiny black eyes, and subtle, rounded ears
cup	yellow ceramic cup with a cute animal face design	a round, ceramic cup with a glossy finish, featuring a wide, cylindrical body tapering slightly towards the top, adorned with a cute cartoon animal face design in shades of yellow, white, and pink, with large brown eyes, a small brown nose, a smiling mouth, and pink cheeks, complemented by a large, smoothly curved handle on the side
slipper	quilted beige slipper with brown trim	a beige quilted slipper with a closed-toe design, featuring a soft, padded upper with a subtle diamond pattern, a smooth tan fabric trim around the opening, a cushioned insole with a matching diamond pattern, and a stitched edge along the sole
plant	green succulent with thick, fleshy leaves	a compact, rosette-shaped succulent plant with thick, fleshy, elongated leaves exhibiting a smooth, matte surface and a muted green color, featuring slightly pointed tips and subtle, natural variegation along the edges
stuffed toy	round plush toy with a beige face, red nose, and brown hat	a round, plush stuffed toy with a soft, tan-colored surface, featuring a circular face with embroidered black eyes, a small red nose, and a smiling black mouth, accented by light pink embroidered cheeks, and adorned with a light brown, textured hat-like rim encircling the top
marker	red and white cylindrical board marker with ridged cap	a cylindrical board marker with a white plastic body featuring bold red text and graphics, including the words "MYPEN Board Marker" and a stylized pen icon, accented by red bands near the ends, a ribbed red cap, and a smooth, glossy surface finish
scrubber	red and green crocheted strawberry-shaped scrubber	a handmade, strawberry-shaped scrubber featuring a vibrant red body with a chunky, knitted texture, accented by a contrasting bright green top resembling leaves, complete with a small loop for hanging, crafted from thick, soft yarn with a slightly fuzzy surface finish

B. Token Learning Strategy

In addition to VAP, we consider a token-based personalization strategy as a natural competitor, inspired by recent work on personalizing vision–language models and image generation models. In this line of work, a new token embedding is learned to represent a user-specific concept, while keeping the backbone model frozen. Methods such as MyVLM (Alaluf et al., 2024) and Yo’LLaVA (Nguyen et al., 2024) follow this paradigm and have shown strong personalization performance in question answering by learning concept tokens with carefully constructed hard and easy negatives.

Directly applying this idea to VLAs, however, is non-trivial. Yo’LLaVA optimizes its concept tokens using a text-based loss on downstream QA, whereas a VLA outputs continuous actions rather than text. To train concept tokens end-to-end for a VLA, one would need to collect personalized manipulation episodes for each user object, which introduces substantial additional data collection overhead. Instead, we adopt a proxy strategy: we first learn concept tokens in a frozen VLM following the Yo’LLaVA recipe, and then transfer the learned token embeddings into the VLA. As we show in the following subsections, the token embedding space changes little between the VLM and the corresponding VLA, making this transfer feasible in practice. We therefore treat token learning as a strong and principled baseline rather than our primary solution, and use the rest of this section to detail how we train the VLMs, analyze the token embedding space, and study the resulting attention patterns.

B.1. Learning Token Embeddings on the Backbone VLM

We closely follow the training pipeline of Yo’LLaVA (Nguyen et al., 2024) when learning personalized tokens in the VLM. Concretely, we start from a frozen PaliGemma 3B model (Beyer et al., 2024), which combines a SigLIP image encoder with a Gemma-based language decoder and is designed for transfer to downstream vision–language tasks. For each personal object, we introduce a new subject identifier token (e.g., `<my_cup>`) into the vocabulary together with a small number of learnable soft tokens. The rest of the VLM parameters, including the vision encoder and language decoder, remain fixed during training.

The personalized token is optimized on a recognition-style VQA dataset rather than on long conversational QA. For each personal object o , we construct yes/no questions of the form “*Can you recognize `<my_cup>` in this image?*” and train the VLM to output a short answer (“*yes*” or “*no*”). This design follows the observation that PaliGemma tends to perform best on short VQA-style prompts and succinct answers; we found that longer conversational templates often led to unstable behavior and mode collapse.

Positive examples use the user-provided reference images of o . For hard negatives, instead of mining from a large external dataset as in Yo’LLaVA (Nguyen et al., 2024), we leverage the actual distractors that appear in our personalized benchmarks. For each distractor instance, we capture more than ten views and label them as hard negatives for the corresponding object token. Easy negatives are sampled from objects that never appear as distractors for o (e.g., props from other tasks), providing a diverse background of unrelated images. This choice is arguably favorable to the token-learning baseline, since the hard negatives are drawn directly from the deployment distribution; nevertheless, our method VAP still substantially outperforms this baseline in personalized manipulation.

Unlike Yo’LLaVA, which represents each subject as a sequence of several learnable soft tokens (e.g., `<my_cup>` is `<token_0><token_1> . . . <token_k>`), we observed that long learned prefixes do not work well with PaliGemma: as k grows, the prompts deviate from the model’s pretraining distribution and the answers become unstable. We therefore learn a single special token embedding for each personal object and place it directly in the question, as in “*Can you recognize `<my_cup>` in this image?*”. During training we freeze all VLM parameters and optimize only this token embedding using a standard cross-entropy loss on the yes/no answers. The resulting embedding lies in the PaliGemma token space and is later copied into the corresponding token embedding matrix of the VLA.

Following Yo’LLaVA, we train each personalized token for 20 epochs using the same optimization hyperparameters as the original method. We monitor performance on a held-out recognition QA set constructed in the same way as the training questions and answers. After training, the VLM attains over 95% accuracy on this validation split for all personal objects, indicating that the learned token reliably captures the visual identity of each object in the VLM’s embedding space.

B.2. Token Embedding Space Analysis

Our proxy strategy relies on the assumption that the token embedding space of the VLM remains largely unchanged when the model is fine-tuned into a VLA. To verify this, we compare the token embeddings of PaliGemma 3B (used as our VLM) with those of the corresponding VLA (π_0 and $\pi_{0.5}$), which is obtained by training on large-scale robotic action data (Intelligence et al., 2025). Both models share the same tokenizer and vocabulary, so their embeddings are aligned by construction.

We extract the token embedding matrices from the text decoders of PaliGemma 3B and each VLA variant, and evaluate their alignment using three metrics: token-wise cosine similarity, linear centered kernel alignment (CKA), and a k-nearest-neighbor top-1 (kNN@1) token matching accuracy. CKA measures how similar the pairwise inner-product structure of two representation spaces is, and equals 1 when one space can be obtained from the other by an orthogonal transformation. The kNN@1 score measures, for each VLM token, whether its nearest neighbor in the VLA embedding space is the corresponding token, thus directly quantifying how often token identities are preserved.

As summarized in Table 8, both π_0 variants are essentially identical to the VLM embeddings: they achieve a mean cosine similarity of 0.999999 ± 0.000000 , a CKA of 1.000000, and a kNN@1 of 0.9998, indicating that almost every token in the VLM embedding matrix is mapped to its exact counterpart in the VLA. The $\pi_{0.5}$ variants still exhibit a high mean cosine similarity of 0.945626 ± 0.066187 , a CKA of 0.985684, and kNN@1 scores between 0.9899 and 0.9913, suggesting that the global geometry of the token embedding space is largely preserved and that token-wise correspondences remain highly stable despite the additional action fine-tuning. Together, these metrics support our approximation that concept tokens learned on the PaliGemma VLM can be transferred to the corresponding VLA without relearning the embedding space from scratch, as they continue to live in essentially the same token embedding space.

These observations are consistent with prior findings on language model fine-tuning, which report that lower layers and embedding matrices change little compared to upper layers during task-specific adaptation (Merchant et al., 2020; Hao et al., 2020). In our context, they suggest that learning personalized tokens on the PaliGemma VLM and then transferring them to the VLA is a reasonable approximation: the token embeddings live in essentially the same space before and after action fine-tuning. This motivates our use of VLM-trained concept tokens as a strong token-learning baseline for personalized manipulation.

Table 8. Token embedding space comparison between PaliGemma-3B (VLM) and various VLA models. All metrics show that the token embedding space remains largely unchanged after fine-tuning the VLM into a VLA, with near-perfect cosine similarity and minimal L2 distance.

Model	Vocab Size	Cosine Similarity	CKA	kNN@1
π_0 (Personalized-SIMPLER Google Robot)	257152	0.999999 ± 0.000000	1.000000	0.9998
π_0 (Personalized-SIMPLER WidowX)	257152	0.999999 ± 0.000000	1.000000	0.9998
$\pi_{0.5}$ (Personalized-VLABench)	257152	0.945626 ± 0.066187	0.985684	0.9913
$\pi_{0.5}$ (Real-world Scenario)	257152	0.945626 ± 0.066187	0.985684	0.9899

B.3. Attention Analysis

In the previous subsections we showed that token learning can successfully fit concept tokens in the VLM and that these tokens transfer almost unchanged into the VLA’s embedding space. A natural question is whether the learned token actually attends to the correct personal object inside the VLA. To probe this, we visualize the spatial attention induced by the learned concept token on the VLA’s visual features.

Concretely, we extract the VLA’s cross-attention weights for the query position corresponding to the learned object token, and take the attention mass over image-token keys as a per-patch score from the last layer (layer 17). We then reshape and resize these scores to the image resolution and normalize them across spatial locations to obtain a heatmap. Intuitively, this heatmap measures how strongly the concept token “recognizes” each region of the image. Figure 9- 12 shows representative examples from Personalized-SIMPLER, overlaid on the original RGB observations.

Across these examples, the learned token *often* assigns higher responses to the personal object than to background regions, indicating that it can bias the VLA’s visual representations toward the user-specified instance. However, we also observe that this localization is frequently *fragile* over time: as the rollout progresses and the robot’s viewpoint and scene

configuration change, the peak activation can shift across frames, sometimes drifting to nearby objects that share similar shape, texture, or category-level cues. Even when the heatmap remains relatively consistent on the target for several steps, the model still exhibits a tendency to select or interact with an incorrect object in cluttered scenes, suggesting that token-induced localization alone does not provide stable, instance-level tracking under continuous, closed-loop execution.

Consistent with our main experiments (Section 5), this instability helps explain why the token-learning baseline does not reliably improve end-to-end manipulation. In particular, the baseline may (i) briefly emphasize the correct object but then drift to a distractor later in the episode, or (ii) maintain reasonable emphasis on the target yet still execute an action on a distractor or fail due to manipulation difficulty. Overall, learned tokens can partially influence where the model “looks,” but the signal is often time-varying and insufficiently discriminative to robustly resolve visually similar instances throughout a multi-step manipulation trajectory.

One plausible explanation for the remaining failures—including episodes where the heatmap appears relatively consistent on the target yet the behavior is still incorrect—is the VLA architecture. The vision–language encoder that produces the text/image embeddings (and contains the learned concept token) is shared with the underlying VLM, whereas the action head is a separate expert trained via flow matching. During action prediction, latent action variables are sampled from noise and attend over the entire sequence of text and image embeddings through cross-attention, mixing information across modalities and tokens. As a result, even when the learned token induces a stable preference in the perceptual representations, this fine-grained, instance-specific cue can be diluted or overridden before it consistently affects the final low-level action distribution. This suggests that, beyond improving token-induced localization, bridging token-level conditioning into reliable instance-aware control in a separate action expert remains challenging.

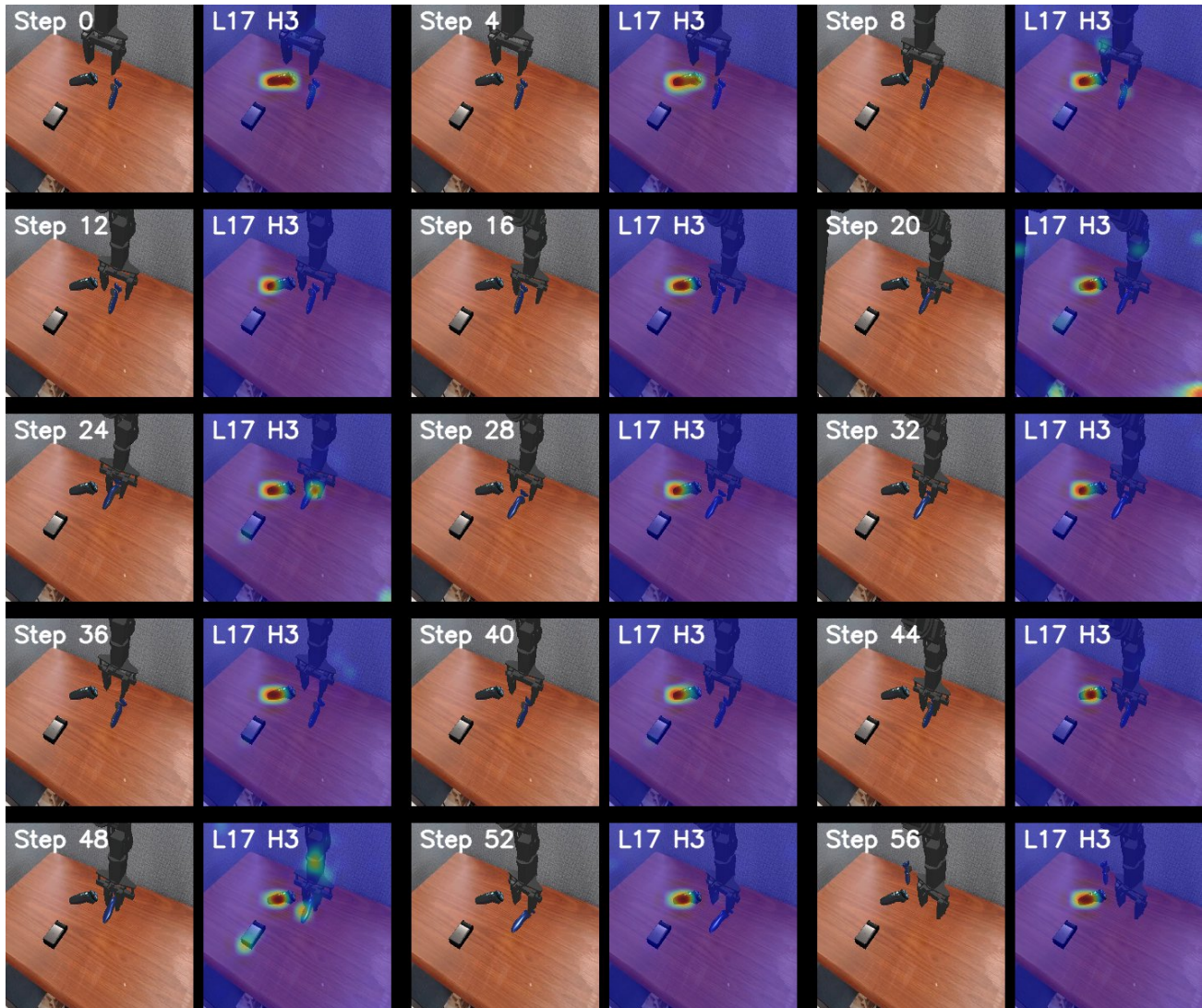


Figure 9. Soft Prompt: relatively consistent localization yet failed execution. Across the rollout, the token-patch similarity heatmaps remain largely concentrated near the intended personal object, but the episode still fails (e.g., incorrect interaction or failure to complete the manipulation), illustrating that correct or stable localization does not necessarily translate into successful control.

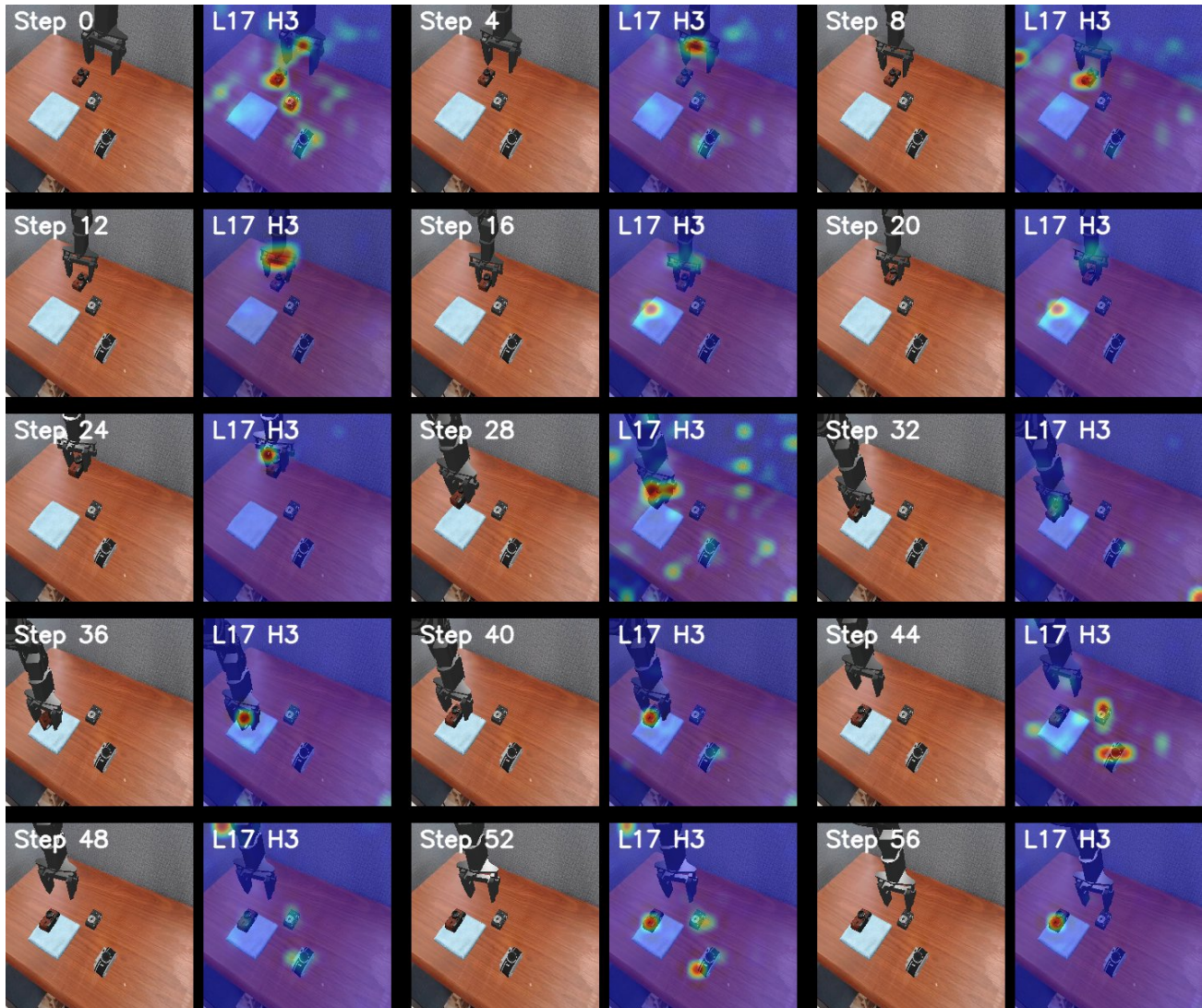


Figure 10. **Soft Prompt: temporally unstable localization.** As the robot moves and the viewpoint changes, the heatmap peaks shift across frames and intermittently activate on different objects/background regions, indicating that the token-induced preference can be fragile over time during closed-loop execution.

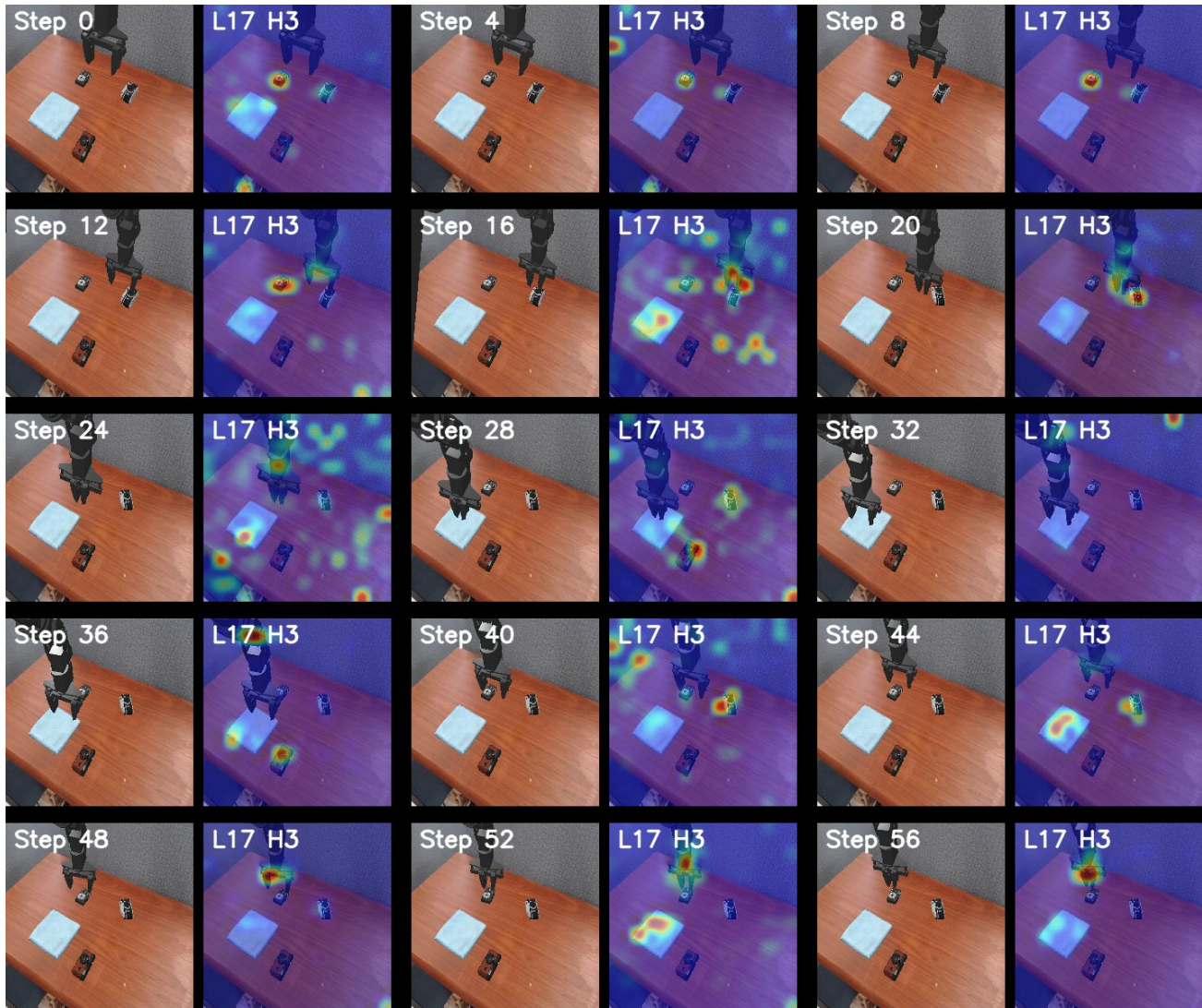


Figure 11. Soft Prompt: confusion under visually similar distractors. In the presence of near-identical instances, the heatmaps show substantial activation on distractors in addition to (or instead of) the target, suggesting that a learned token often provides only a coarse instance bias and may not reliably disambiguate visually similar objects.

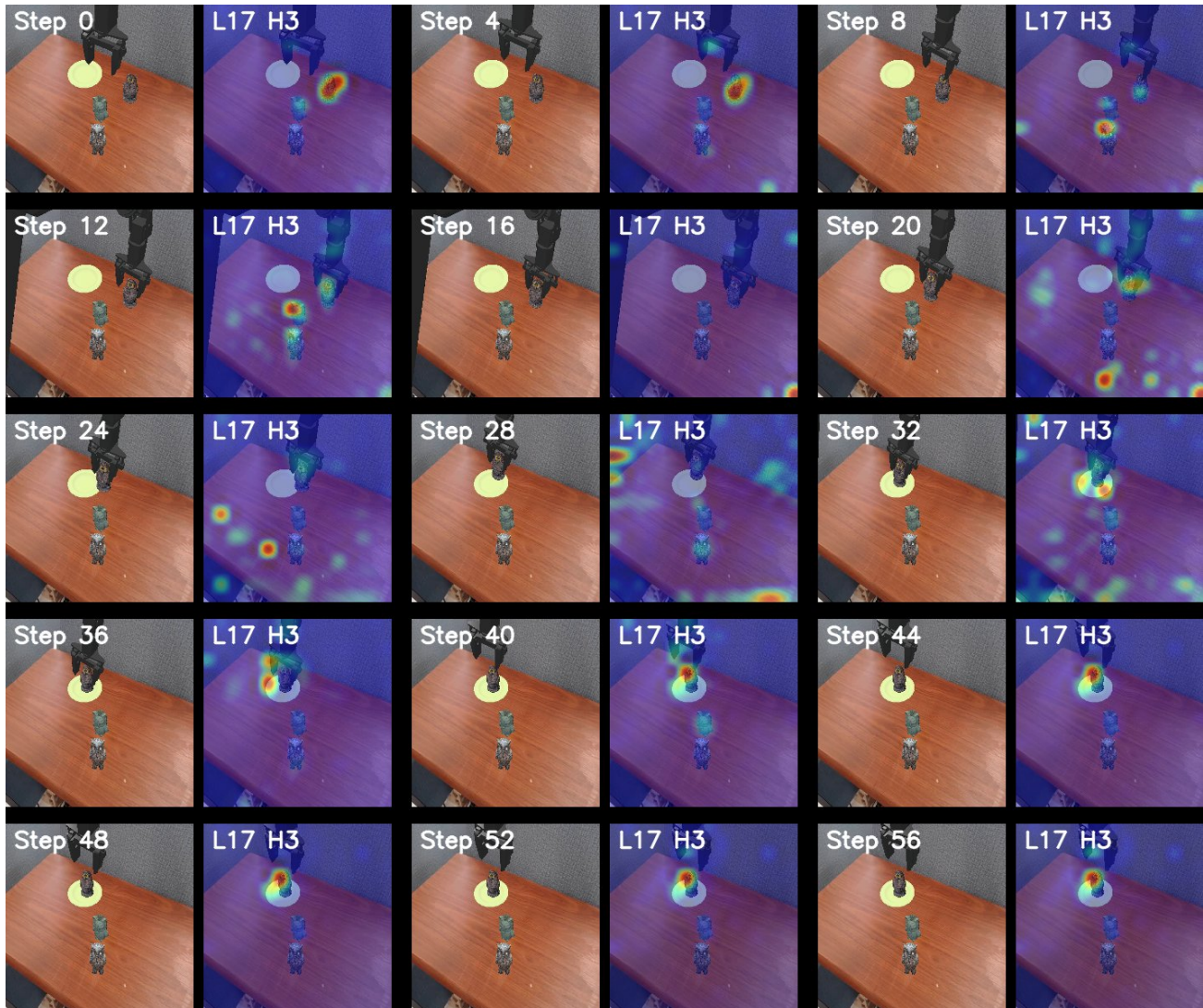


Figure 12. **Soft Prompt: a successful episode.** This example shows a case where the heatmaps place comparatively higher responses on the intended personal object across the rollout and the task succeeds, highlighting that token learning can sometimes provide useful instance bias, albeit not consistently across scenes and time.

C. Qualitative Examples

In this section, we present additional qualitative examples that illustrate how VAP behaves in practice. For each task in each benchmark, we show representative rollouts where the agent successfully identifies and manipulates the user’s personal object among visually similar distractors. For each rollout, we visualize all frames of the episode, including the generated visual prompts overlaid on the input images.

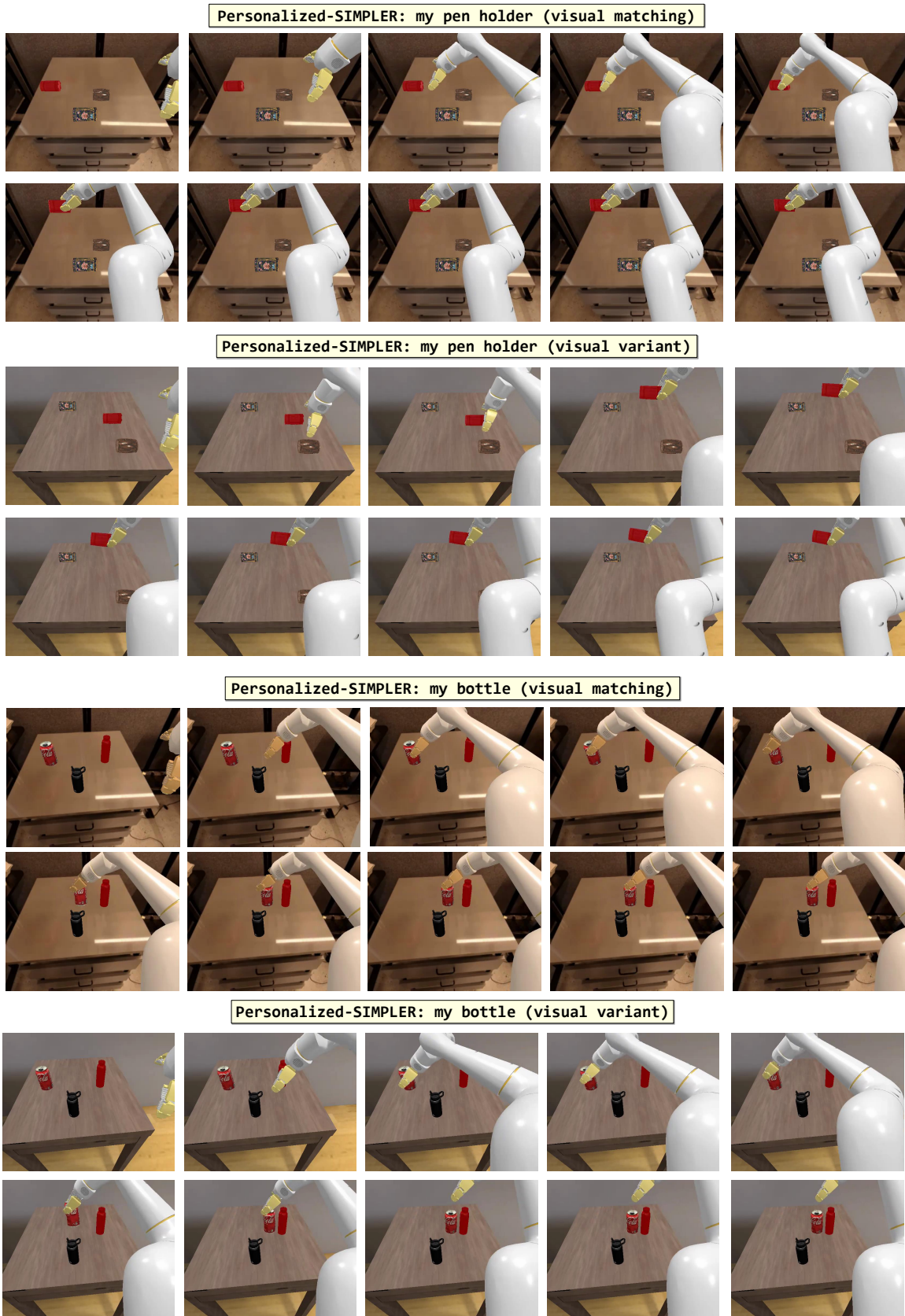


Figure 13. Qualitative Examples on Personalized-SIMPLER (Google Robot)

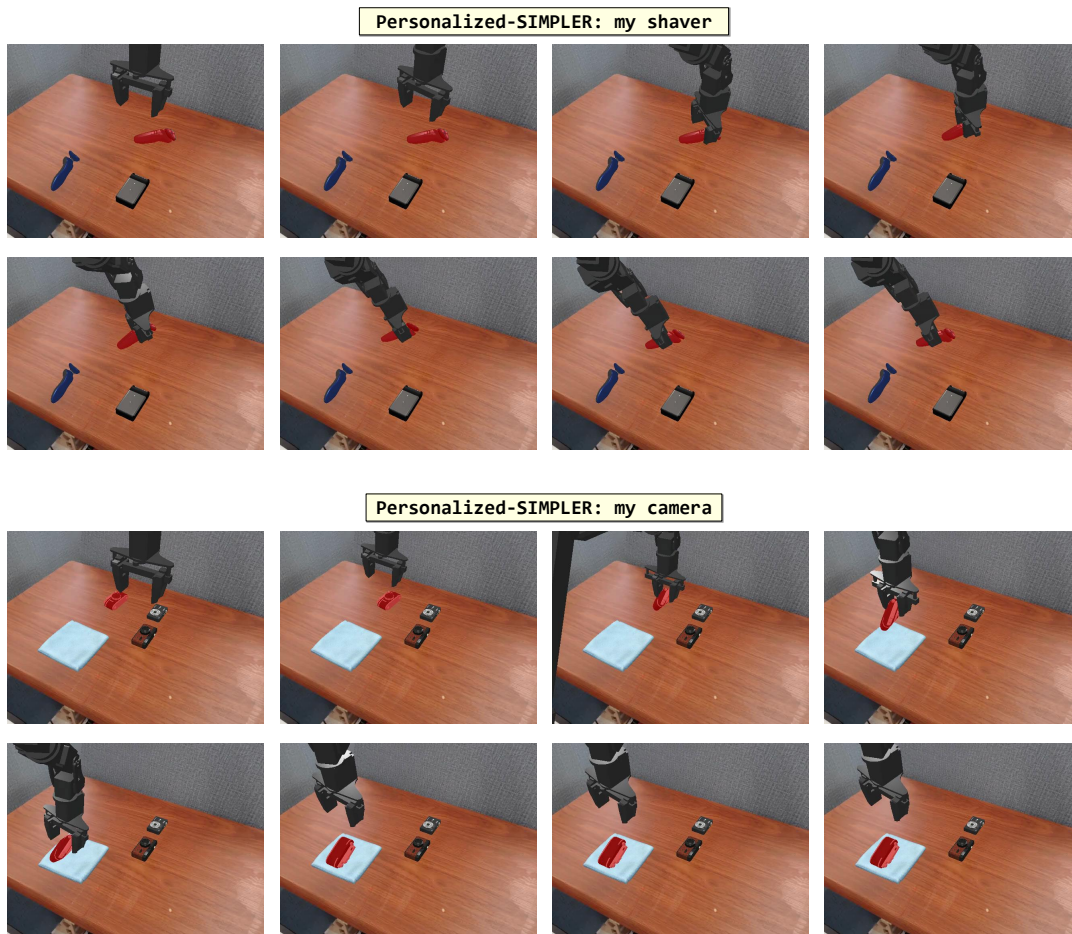


Figure 14. Qualitative Examples on Personalized-SIMPLER (WidowX) - 1

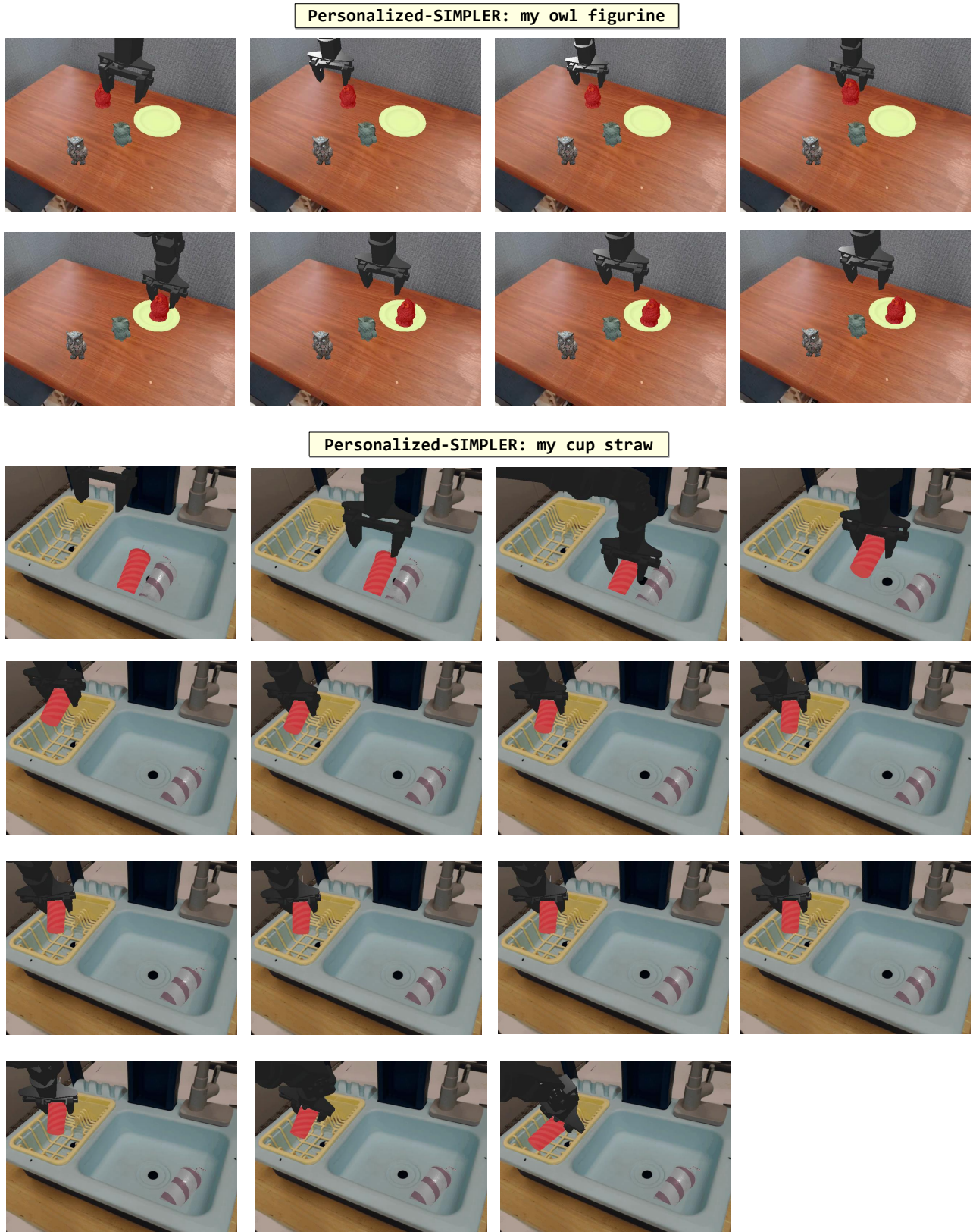


Figure 15. Qualitative Examples on Personalized-SIMPLER (WidowX) - 2

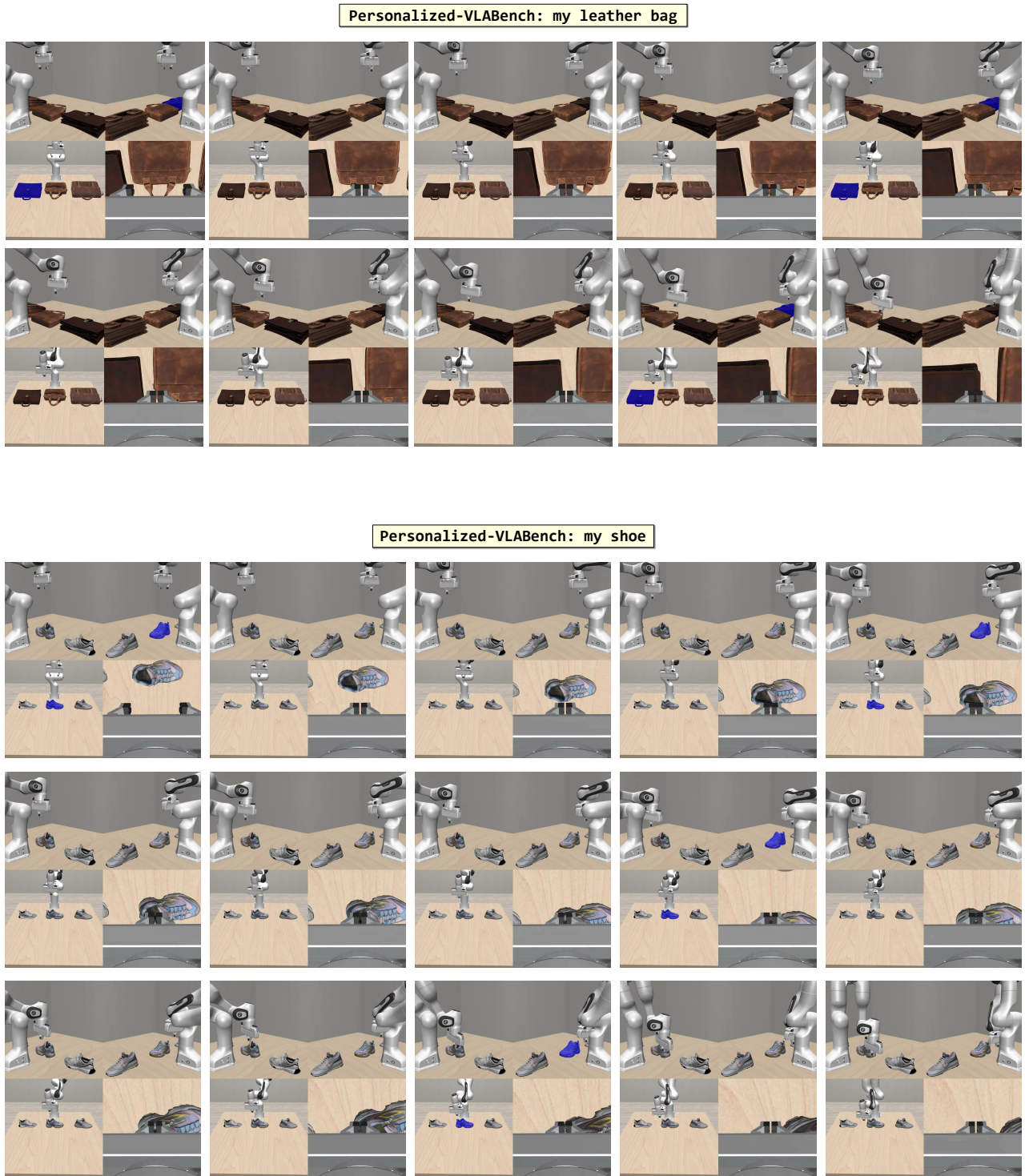
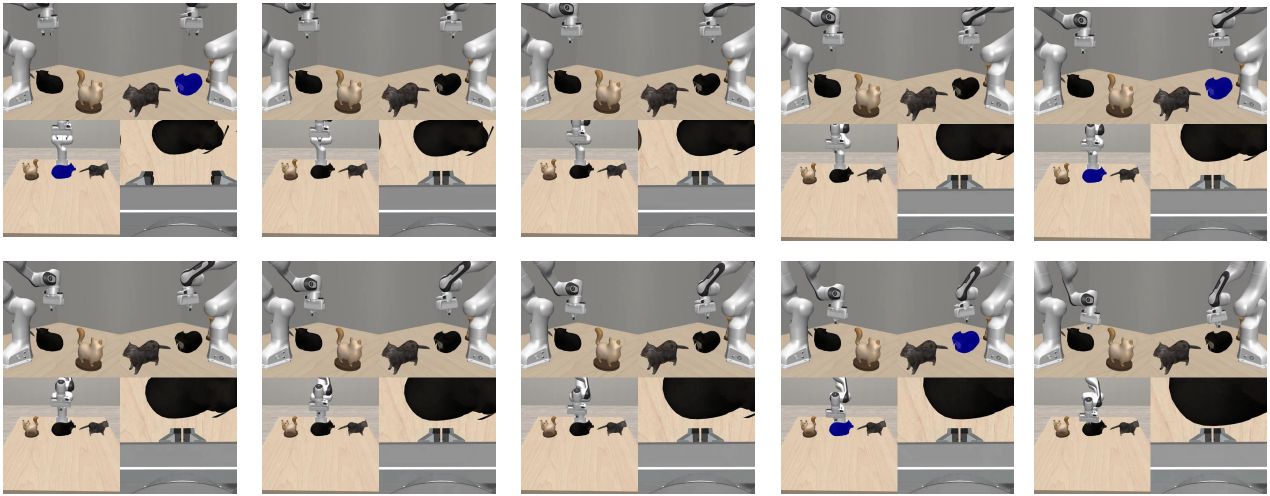
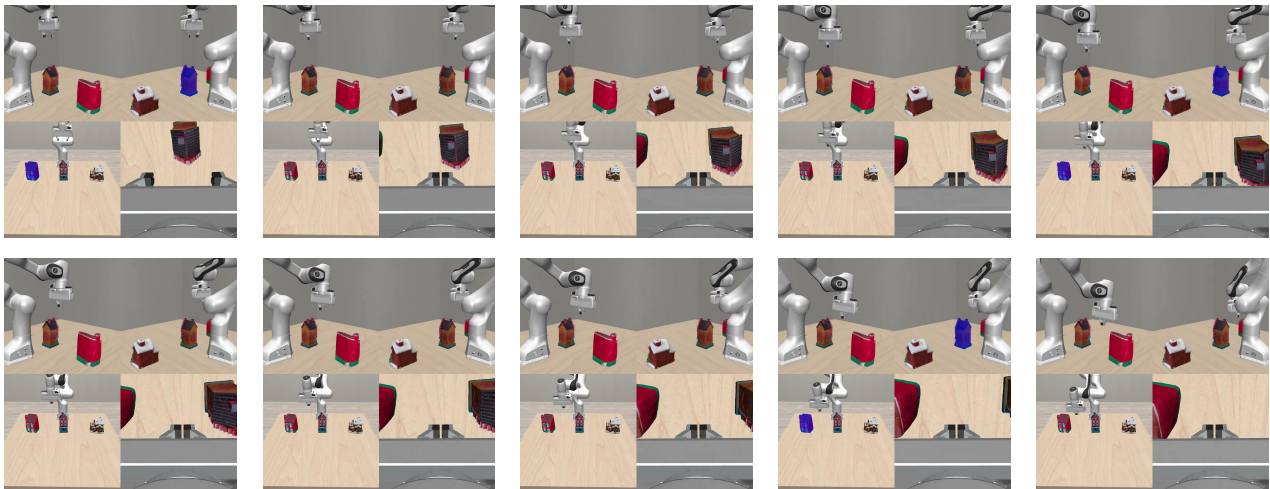


Figure 16. Qualitative Examples on Personalized-VLABench - 1

Personalized-VLABench: my cat figurine



Personalized-VLABench: my miniature house



Personalized-VLABench: my cup

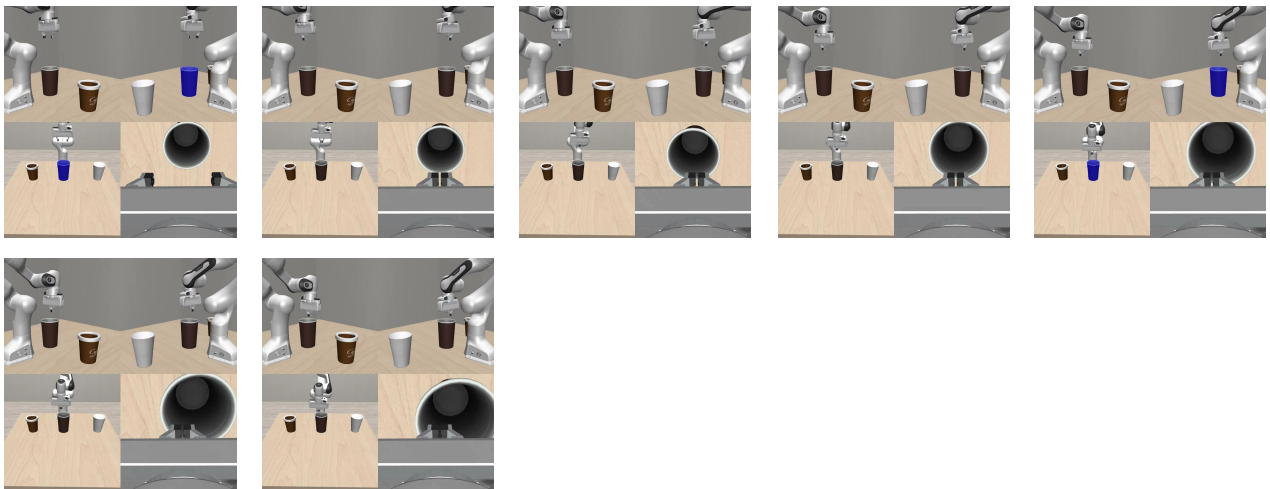


Figure 17. Qualitative Examples on Personalized-VLABench - 2

D. Error Case Analysis

While VAP substantially improves personalized manipulation success, it still fails in certain characteristic ways. In this section, we categorize typical failure modes and provide qualitative examples for each. Beyond illustrating representative roll-outs, these cases help disentangle whether failures primarily stem from the upstream perception/prompting pipeline or from the downstream VLA behavior under challenging manipulation dynamics. As summarized in Table 9, failures in single-view settings are less often due to wrong prompts (Case 1: 13.1%/21.4% of failures in Fractal/Bridge), whereas multi-view settings are dominated by cross-view inconsistencies (Case 2: 59.2%/50.9% of failures in Personalized-VLABench/Real-world). We group errors into three types: (1) incorrect visual prompts arising from single-view ambiguity, (2) inconsistent prompts across multiple views, and (3) correct prompts that nonetheless do not lead to successful actions from the VLA. Figures 18–20 show representative examples for each category; they are intended to illustrate the taxonomy rather than provide an exhaustive survey of failures.

D.1. Case 1: Wrong Visual Prompt (Single View)

In the first category, the perception pipeline produces an incorrect mask for the personal object even though only a single camera view is involved (13.1%/21.4% of failures in Fractal/Bridge; Table 9). We observe two common sub-cases: (i) the open-vocabulary detector incorrectly localizes the *generic* class in a cluttered scene (e.g., producing an imprecise or shifted box/mask that already excludes the true instance), and (ii) the open-vocabulary detection is reasonable but the subsequent image-encoder matching assigns a higher similarity score to a distractor than to the ground-truth personal instance (i.e., the top-1 retrieval is wrong). The latter can occur even when the target is visible, particularly when multiple near-identical instances exist and the reference set does not capture the most discriminative view. In such cases, the selected visual prompt can remain stable yet consistently highlight the wrong object throughout the episode; the failure is therefore rooted in the grounding function g , and the VLA simply and consistently acts on the object it is shown. This also suggests a concrete direction for improvement: adapting or training the image encoder to better separate *personalized* instances (e.g., instance-discriminative matching) could reduce retrieval-induced prompt errors without changing the downstream VLA (see Figure 18).

D.2. Case 2: Wrong Visual Prompt (Multi-View Inconsistency)

The second category arises from inconsistencies across camera views and accounts for a large fraction of failures in multi-view settings (59.2% in Personalized-VLABench and 50.9% in Real-world; Table 9). Even when each individual view is moderately informative, per-view matching and tracking can occasionally lock onto different objects in different cameras, especially under severe occlusion, partial visibility in the wrist camera, or extreme viewpoint changes that alter apparent shape/texture. This produces multi-view scenes where one camera correctly highlights the personal object, while another highlights a distractor, yielding conflicting prompts that can destabilize behavior or bias actions toward the wrong view. These cases expose a limitation of our current per-view grounding design and motivate future work on explicitly enforcing cross-view consistency. For example, recent cross-view correspondence/segmentation work such as ObjectRelator introduces mechanisms for cross-view object alignment across ego-/exo-centric perspectives that may provide useful building blocks for reducing Case 2 failures in our setting (Fu et al., 2025) (see Figure 19).

D.3. Case 3: Correct Visual Prompt but Failed Manipulation

In the third category, the visual prompt correctly highlights the personal object in all relevant views, yet the agent still fails the manipulation task (Case 3 accounts for 86.9%/78.6% of failures in Fractal/Bridge and 40.8%/49.1% in Personalized-VLABench/Real-world; Table 9). Qualitatively, we often observe that the robot approaches the visually prompted object (indicating that the prompt successfully resolves instance identity), but the episode still fails due to manipulation difficulty—e.g., tight grasps, clutter-induced collisions, or precise placement requirements where small execution errors accumulate. In these examples, improving grounding alone is unlikely to close the remaining gap: success appears limited by the VLA’s underlying manipulation capability and robustness under contact-rich, cluttered dynamics. This points to a complementary direction—strengthening the VLA itself (e.g., better base policy competence or robustness)—to convert correct instance conditioning into reliably successful end-to-end manipulation (see Figure 20).

Bring My Cup! Personalizing Vision-Language-Action Models with Visual Attentive Prompting

Benchmark	Setting	#Eps	Fail (%)	Case 1 (%)	Case 2 (%)	Case 3 (%)
Personalized-SIMPLER (Fractal)	Google Robot (1 view)	1,685	37.6	13.1	—	86.9
Personalized-SIMPLER (Bridge)	WidowX (1 view)	96×10	16.6	21.4	—	78.6
Personalized-VLABench	Franka (3 views)	125×10	38.4	—	59.2	40.8
Real-world	SO-101 (3 views)	20×8	31.9	—	50.9	49.1

Table 9. Error-mode breakdown for VAP across benchmarks with more details. “Fail (%)” is computed over all evaluation episodes. Case 1–3 are computed *conditional on failure* and should sum to 100% within each row. Case 2 (multi-view inconsistency) is not applicable to single-view settings and Case 1 (single-view ambiguity) is not applicable to multi-view settings.

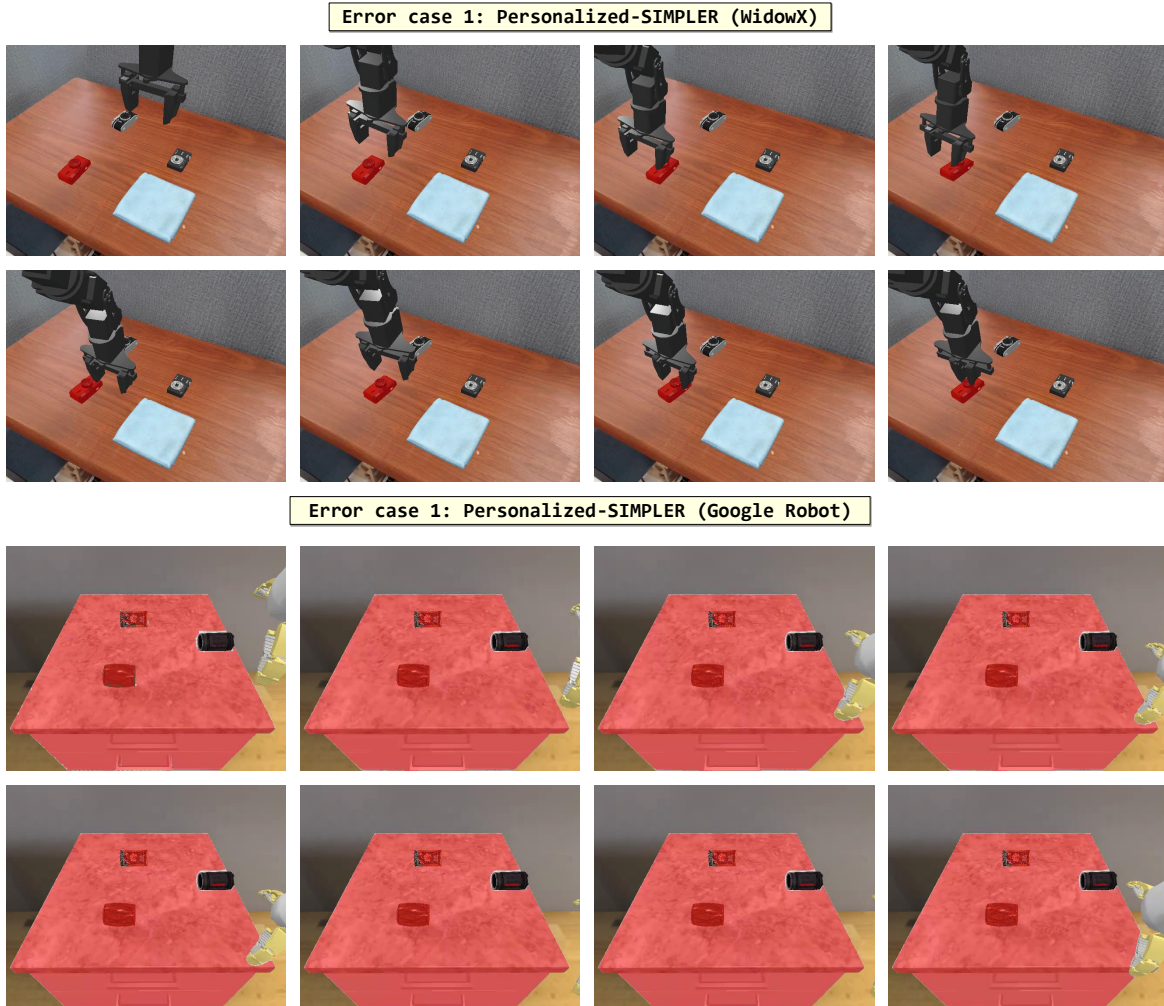


Figure 18. **Case 1 (single view): wrong visual prompt due to grounding/matching error.** The open-vocabulary detector proposes a plausible region for the generic class, but the instance-level matching selects a distractor whose embedding similarity exceeds that of the true personal object; the resulting mask consistently highlights the wrong instance, and the robot correspondingly interacts with the distractor.

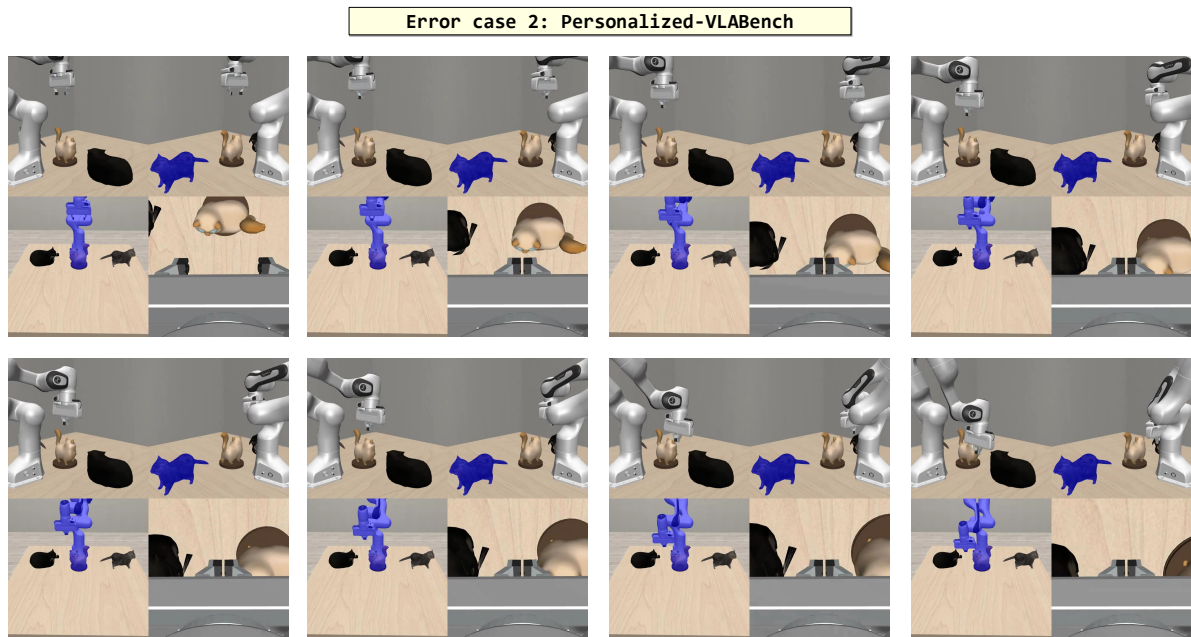


Figure 19. **Case 2 (multi-view): inconsistent visual prompts across cameras.** Per-view grounding/tracking locks onto different instances in different views (e.g., the target in one camera but a distractor in another), yielding contradictory mask prompts; this cross-view inconsistency leads to unstable or biased actions toward the wrong view/object.

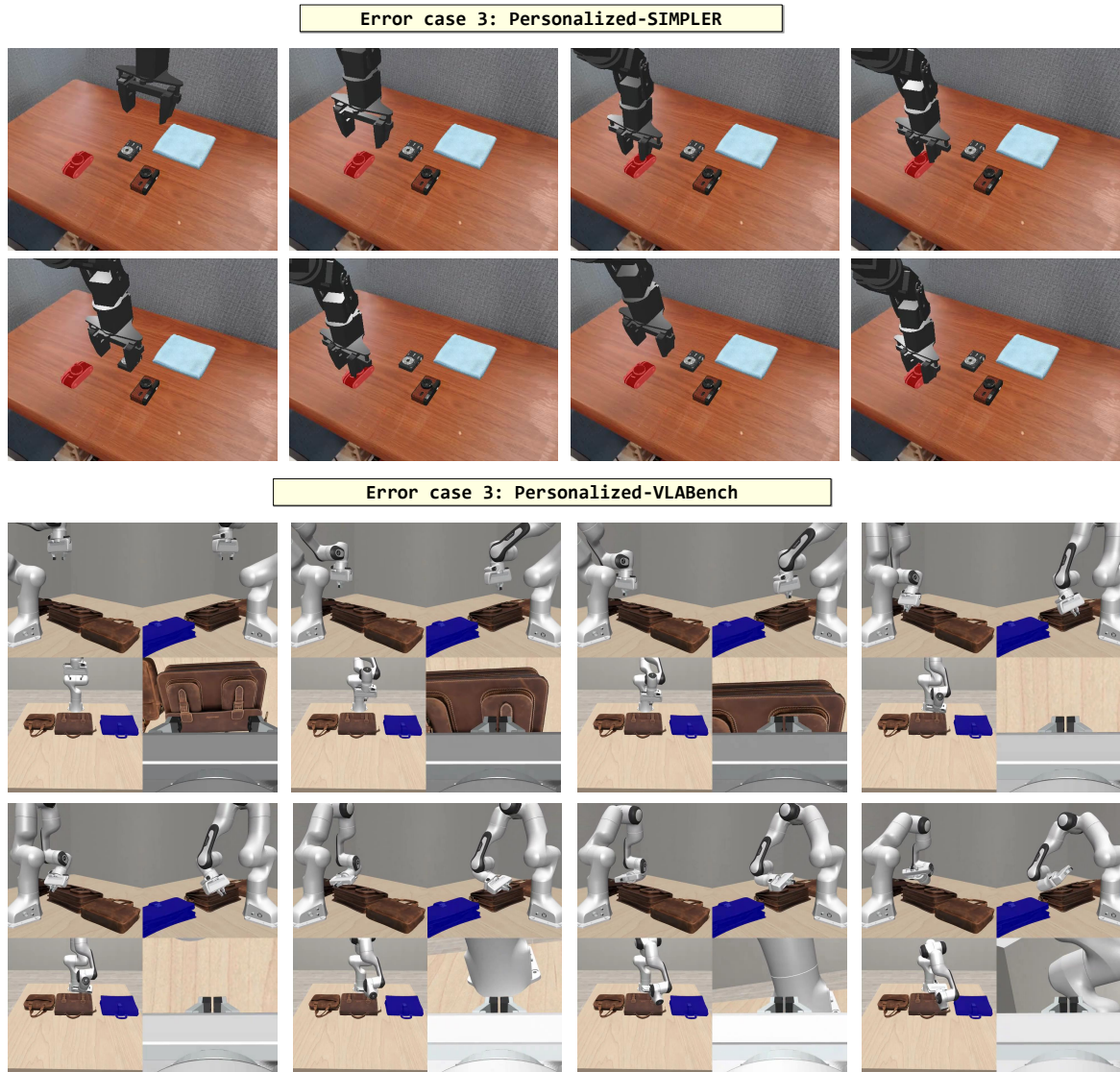


Figure 20. **Case 3 (correct prompt): correct instance highlighted but manipulation fails.** The mask prompt consistently highlights the intended personal object in all relevant views, and the robot approaches the prompted object, yet the episode fails due to challenging contact-rich manipulation (e.g., tight grasps, clutter-induced collisions, or precise placement tolerances), suggesting a limitation of the underlying VLA policy rather than grounding.

E. Discussion and Future Directions

VAP is a training-free framework that personalizes pre-trained Vision–Language–Action models for user-specific robotic manipulation by augmenting them with a modular front-end for personal-object recognition and instruction rewriting. Across two simulation benchmarks and a real-world robotic arm, VAP substantially improves instance-level success over non-personalized and token-based baselines. Our current instantiation is scoped to tabletop scenes with a single personalized object and short-horizon tasks, and it relies on off-the-shelf open-vocabulary detection and segmentation to provide accurate masks. When grounding is incorrect or inconsistent across camera views, these errors propagate to the visual prompts and can lead to failures (Appendix D). We view these aspects not as fundamental obstacles, but as concrete axes along which VAP can be strengthened—for example by incorporating stronger cross-view 3D grounding, lightly adapting the action head to better exploit visual prompts, and combining our module with planners that reason over sequences of personalized sub-tasks.

Even at the level of object manipulation, there is substantial room to expand what personalization means. It is not only about *which* object to handle, but also *how* to handle it: one user may prefer that their mug is always grasped by the handle, that their laptop is never lifted by the screen, or that a fragile plant is moved only by supporting the pot from below. These preferences are naturally expressed as user-specific affordance maps over personal objects, conditioning not just the target but the contact locations, approach directions, and allowable forces. Beyond inanimate objects, users may ask robots to “take care of my cat” or “be gentle with my child’s favorite plush toy,” which requires combining personalization with safety- and comfort-aware interaction models. Extending VAP to learn such affordance-level preferences from a small number of demonstrations or corrections is a promising direction.

Looking further ahead, we see personalized manipulation as one component of a broader ecosystem of user-centered robots. Ideas from VAP could be used to personalize spatial conventions (e.g., learning what “my side of the desk” or “where my keys usually go” means for each user), to restore a preferred workspace layout after cleaning, or to execute multi-step routines such as “set up my desk for work” or “reset the living room for movie night”. As robots move into shared homes and offices, personalization may also need to reconcile competing preferences across multiple users and devices, and to generalize personal concepts across embodiments (phones, desktop agents, mobile robots) while retaining on-device, training-free adaptation for privacy and responsiveness. Incorporating additional modalities such as speech, prosody, gaze, touch, and even physiological signals could help capture subtler forms of intent, comfort, and trust. At the same time, any such system must respect boundaries around what counts as “personal”, provide transparency and control over stored references, and degrade gracefully when users update or revoke their preferences. We hope that VAP can serve as a simple mechanism for injecting user-specific signals into large VLAs, and that future work will build on this to personalize not only objects, but also concepts, routines, and long-term interactions in a safe and trustworthy way.